

MAGNETIC HELICITY IN THE SOLAR ATMOSPHERE: MUCH GAINED, STILL A LOT TO LEARN

MANOLIS K. GEORGOULIS

RCAAM OF THE ACADEMY OF ATHENS

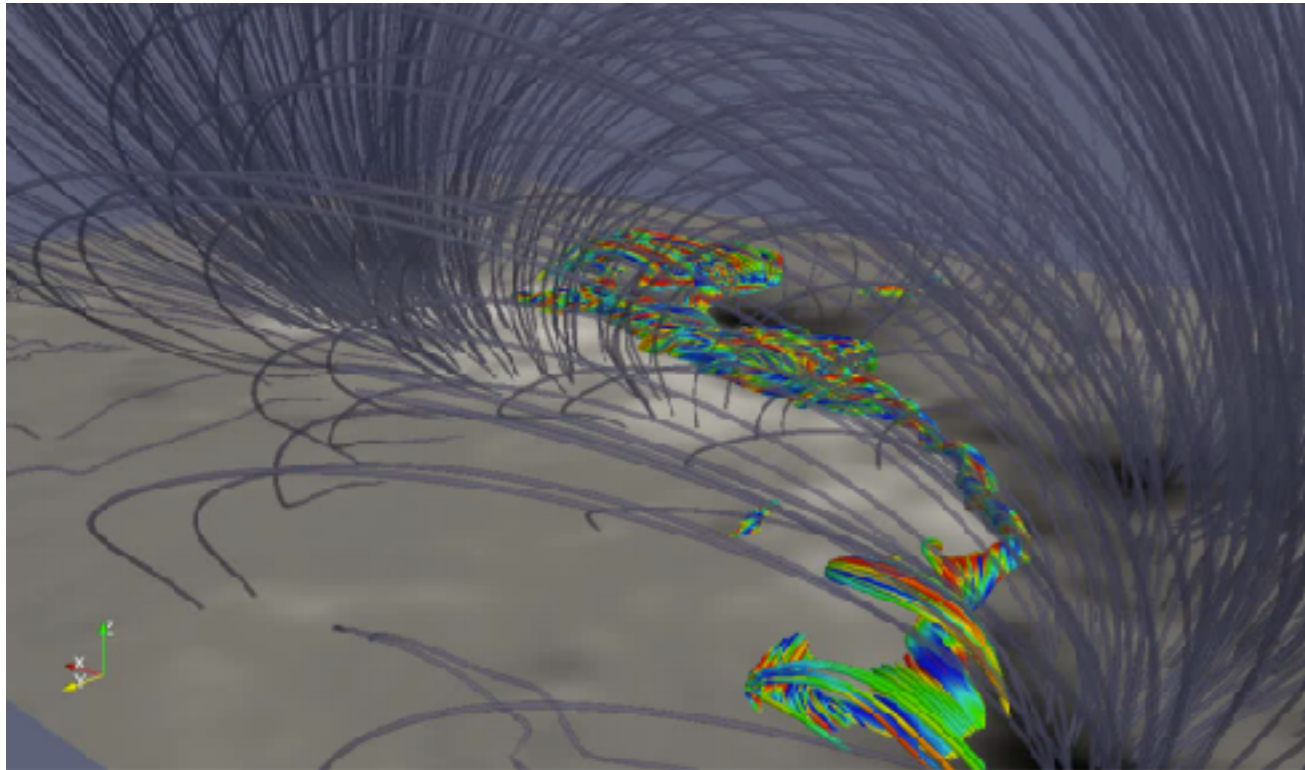
From Pioneering Thinking and Reasoning ...

- Gauge-invariance theorem by Woltjer (1958) $\int_V \mathbf{A} \cdot \text{curl } \mathbf{A} dV = \text{constant},$
- Taylor's min-energy works in the seventies (1974, 1976)
- Mitch's decompositions / flux calculations in the eighties (1984)
- N. Seehafer's current helicity in 1990
- Calugareanu invariant of Moffatt & Ricca (1992)
- Assertion on CMEs by B. C. Low (1994)
- Alexei's major observational finding in 1995
- D. Rust's and A. Kumar's works in 1996
- D. Canfield's and co. work on sigmoids in 1999

Many researchers in the 2000s and 2010s, aiming toward a practical calculation: H. Zhang, K. Kusano, P. Demoulin, A. Nindos, B. J. LaBonte, M. Zhang, K. Kuzanyan, E. Pariat, G. Valori, S. Regnier, J. Thalmann, A. Yeates, Y. Guo ...

… to Recent Developments

- Formation of helical magnetic flux ropes prior to eruptions



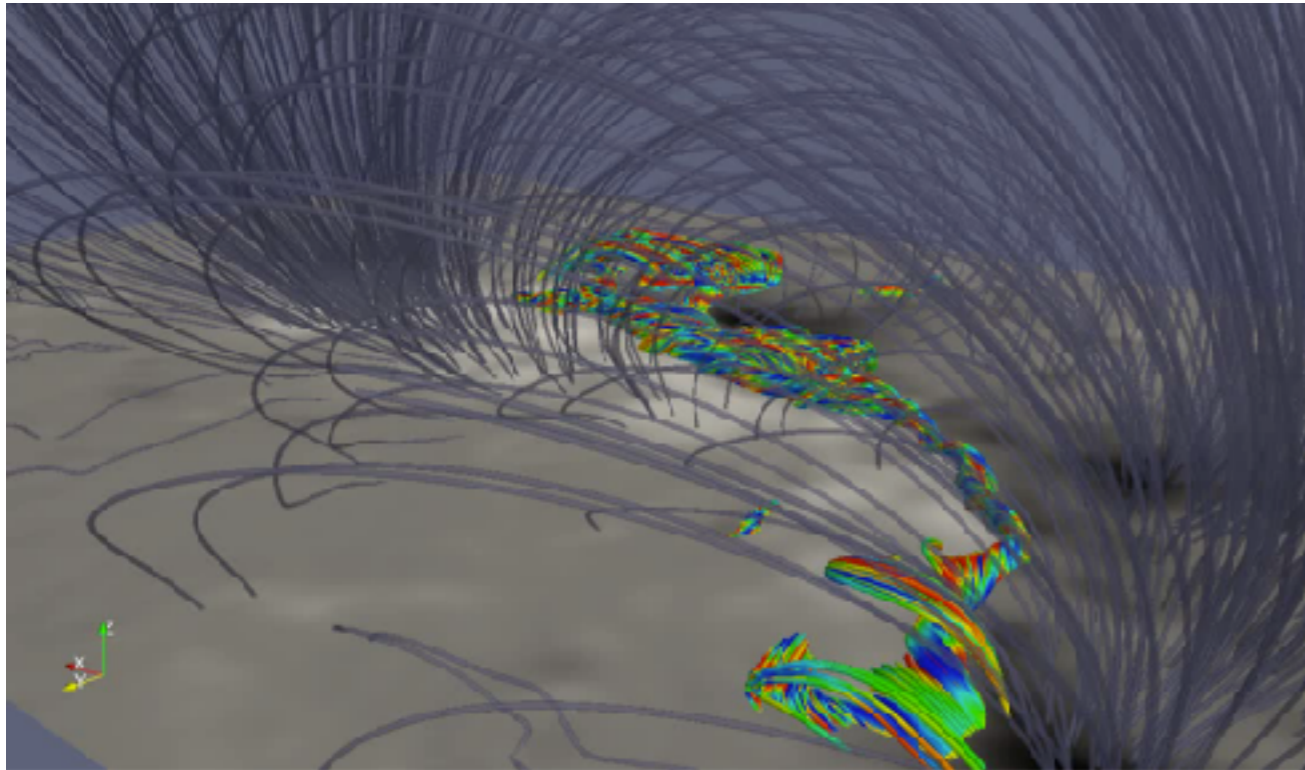
Courtesy: George Chintzoglou (LMSAL)

Also, Chintzoglou et al., (2015);
Nindos et al., (2015)

(see also works on helical flux ropes by S. Gibson)

… to Recent Developments

- Formation of helical magnetic flux ropes prior to eruptions



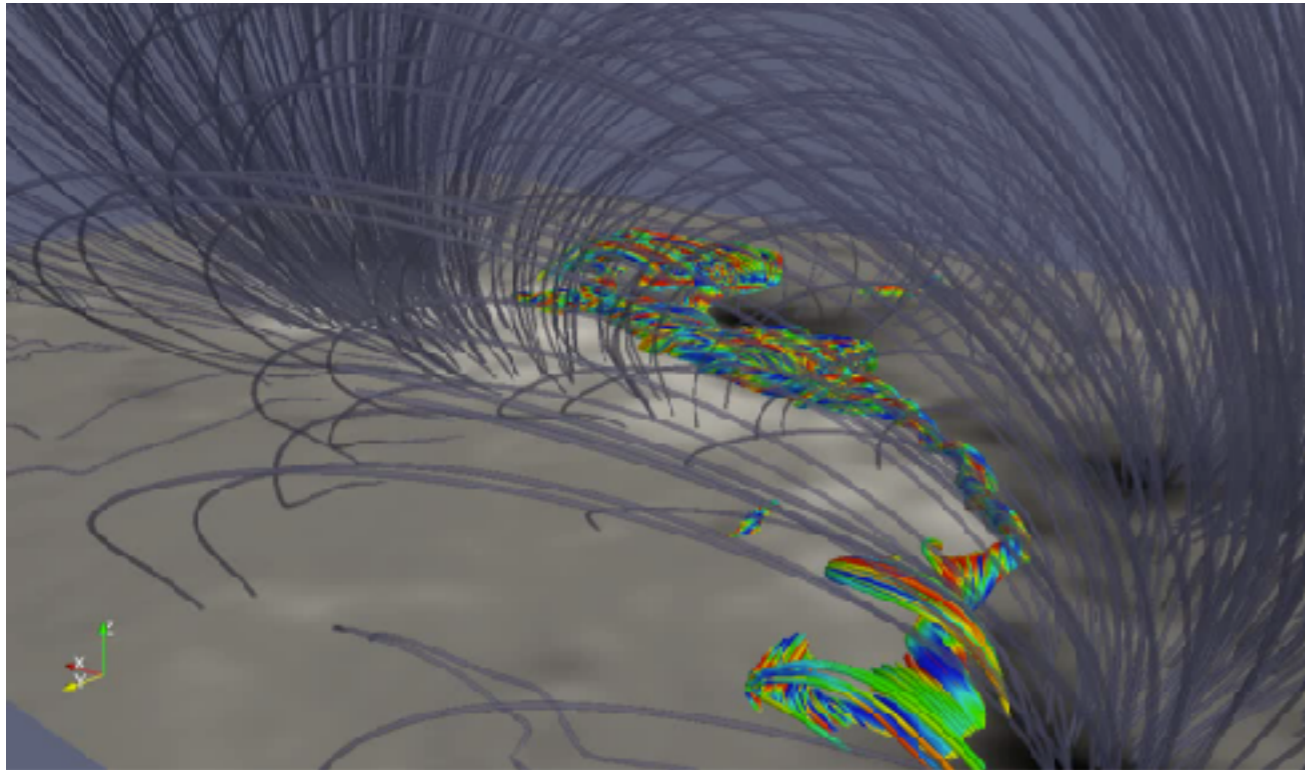
Courtesy: George Chintzoglou (LMSAL)

Also, Chintzoglou et al., (2015);
Nindos et al., (2015)

(see also works on helical flux ropes by S. Gibson)

... to Recent Developments

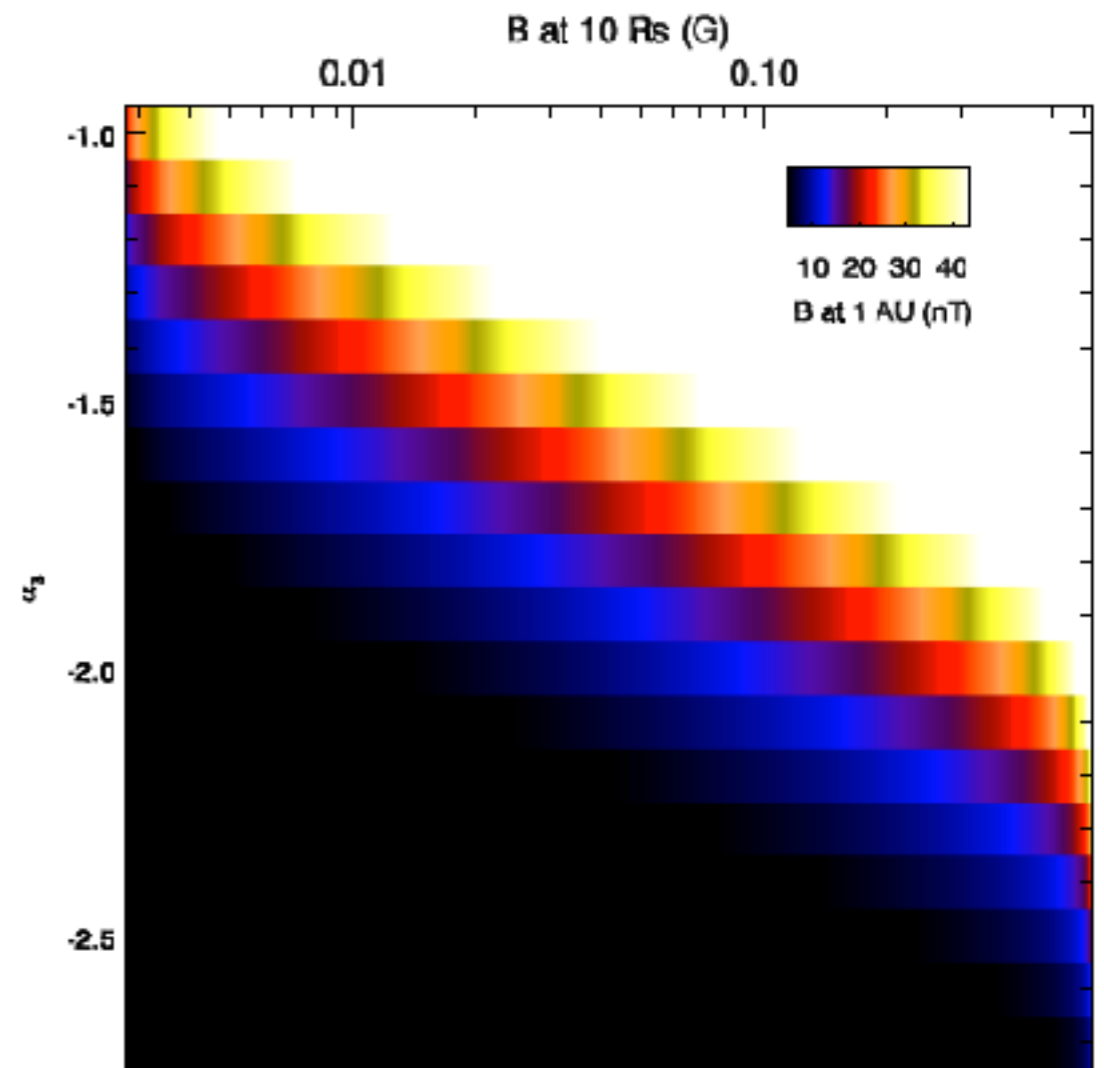
- Formation of helical magnetic flux ropes prior to eruptions



Courtesy: George Chintzoglou (LMSAL)

Also, Chintzoglou et al., (2015);
Nindos et al., (2015)

- Conservation of magnetic helicity in CMEs and extrapolation to get the CME B_z at L1



Patsourakos & Georgoulis (2016)

(see also works on helical flux ropes by S. Gibson)

Instantaneous Magnetic Helicity Budget vs. Helicity Injection Rate

- Knowledge of the 3D field above a boundary allows inference of the helicity budget

$$H = \int_V \mathbf{A} \cdot \mathbf{B} dV \quad \begin{array}{l} \text{gauge-} \\ \text{dependent in} \\ \text{general} \end{array}$$

- Subtracting the reference helicity from the potential field, allows calculation of the relative magnetic helicity

$$H = \int_V (\mathbf{A} + \mathbf{A}_p) \cdot (\mathbf{B} - \mathbf{B}_p) dV$$

and alternative approaches, such as the field-line helicity (e.g., Aly, FDR, Lowder & Yeates, 2017)

$$\mathcal{A}(L) = \int_{L(x)} \frac{\mathbf{A} \cdot \mathbf{B}}{|\mathbf{B}|} d\ell$$

Instantaneous Magnetic Helicity Budget vs. Helicity Injection Rate

- Knowledge of the 3D field above a boundary allows inference of the helicity budget

$$H = \int_V \mathbf{A} \cdot \mathbf{B} dV \quad \begin{array}{l} \text{gauge-} \\ \text{dependent in} \\ \text{general} \end{array}$$

- Subtracting the reference helicity from the potential field, allows calculation of the relative magnetic helicity

$$H = \int_V (\mathbf{A} + \mathbf{A}_p) \cdot (\mathbf{B} - \mathbf{B}_p) dV$$

and alternative approaches, such as the field-line helicity (e.g., Aly, FDR, Lowder & Yeates, 2017)

$$A(L) = \int_{L(x)} \frac{\mathbf{A} \cdot \mathbf{B}}{|\mathbf{B}|} d\ell$$

- On the other hand, knowledge of the velocity field and the magnetic field vectors on the boundary plane allows evaluation of the Poynting theorem for relative magnetic helicity (e.g., Berger & Field, 1984; Kusano et al., 2002)

$$\frac{dH}{dt} = 2 \int_S \mathbf{A} \times (\mathbf{u} \times \mathbf{B}) \cdot \hat{\eta} dS$$

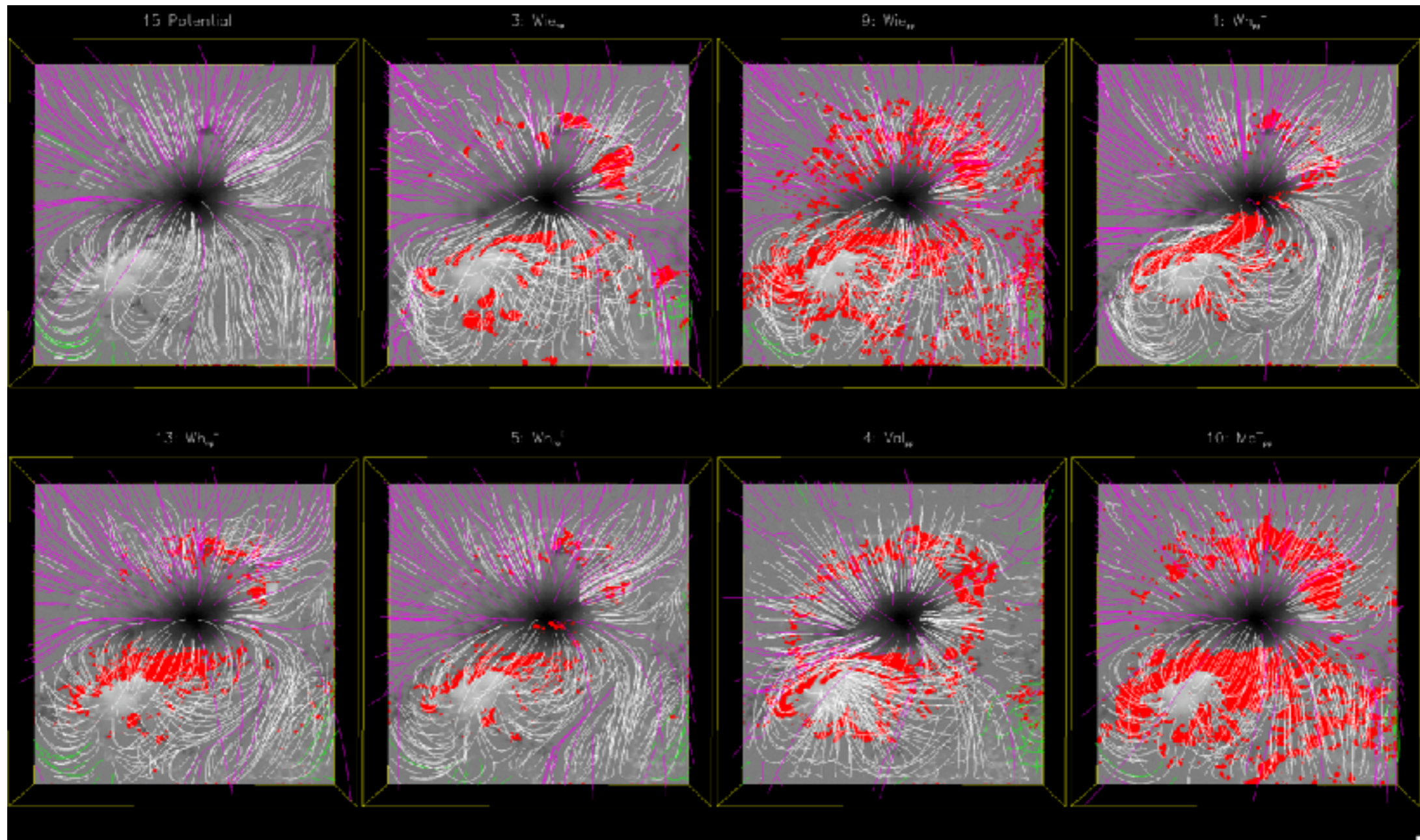
and its practical implementation by Demoulin & Berger (2003):

$$\frac{dH}{dt} = -2 \int_S (\mathbf{A}_p \cdot \mathbf{u}_{ct}) B_n dS$$

- Then the relative helicity is obtained by time integration of (dH / dt)

However, there are Caveats and Shortcomings in Both Approaches

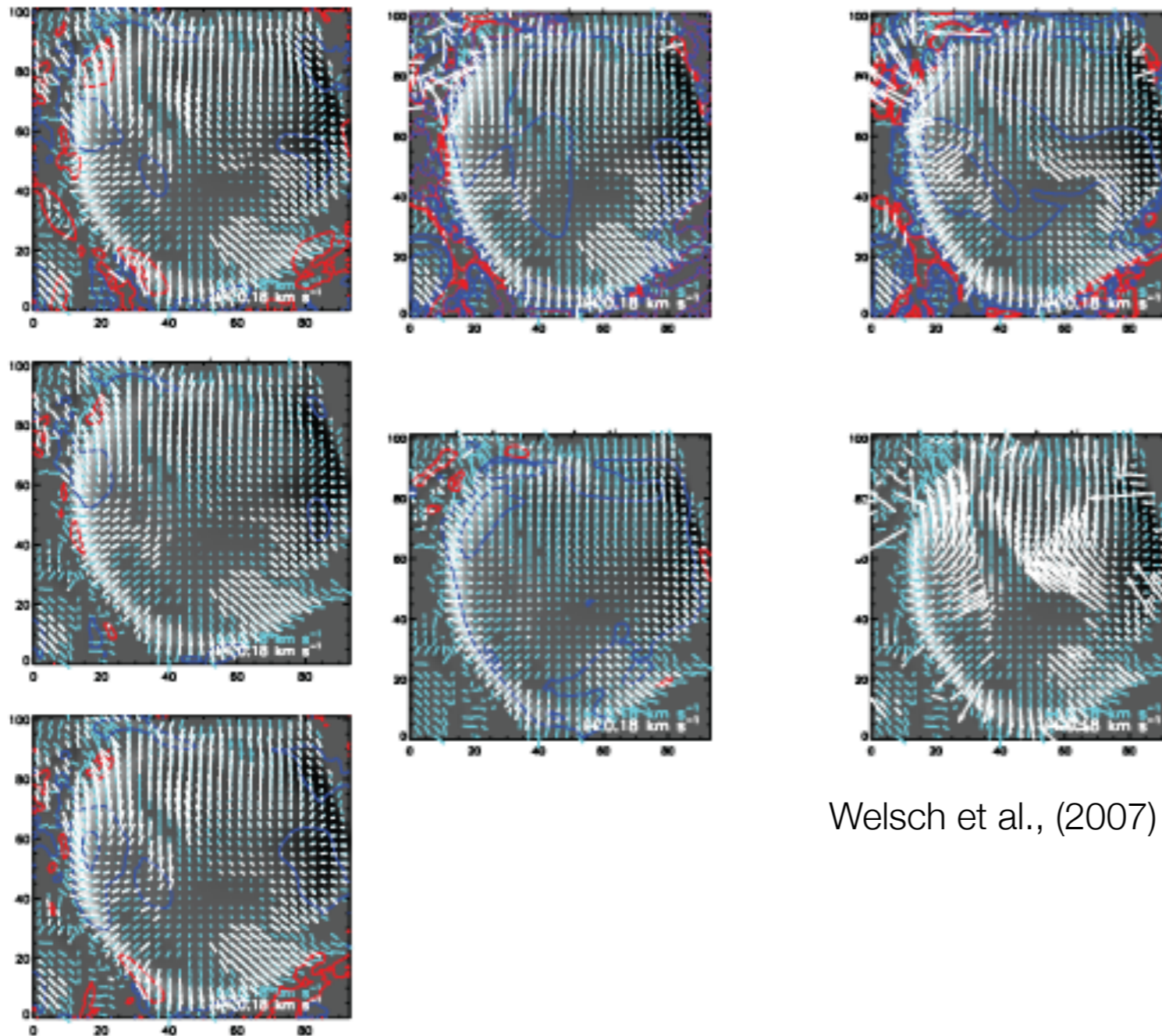
- The unmeasured coronal field is ambiguous and non-unique from 3D field extrapolations, thus having an unknown effect on helicity



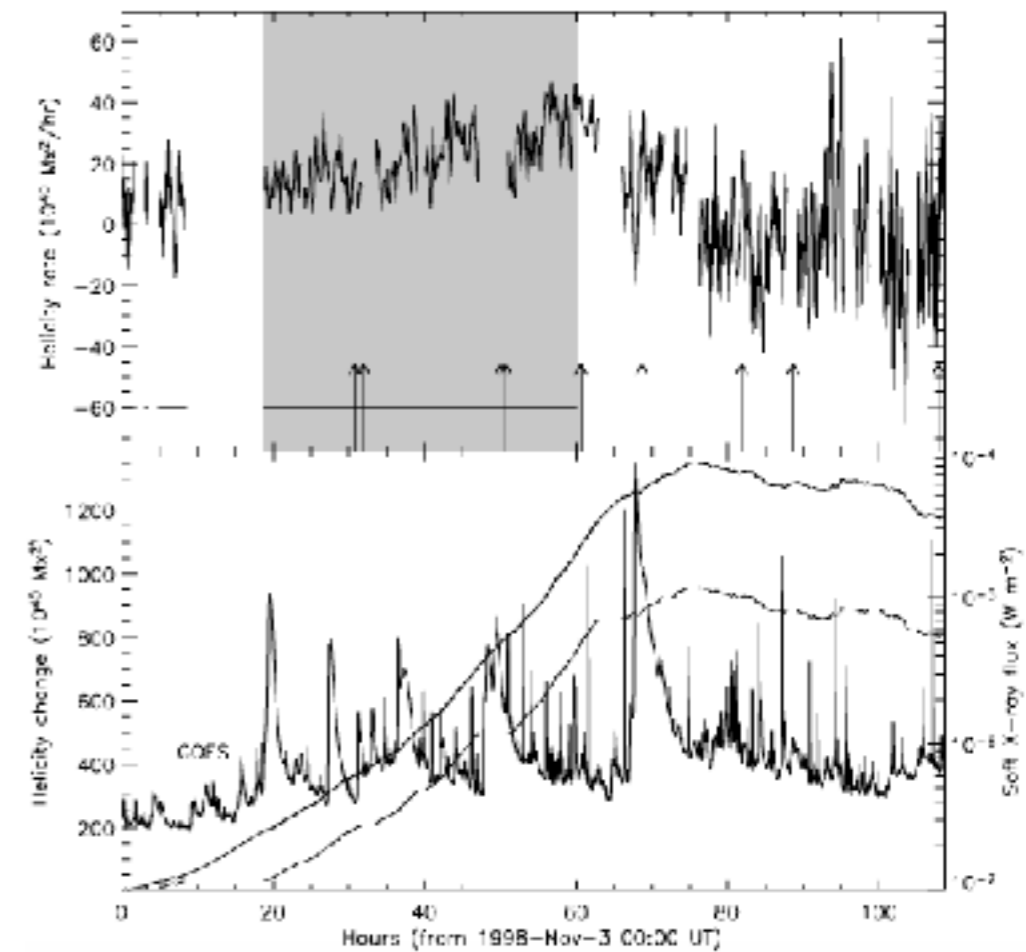
Schrijver et al., (2008)

However, there are Caveats and Shortcomings in Both Approaches

- ... while the velocity field vector on the boundary is also unknown and ambiguous, plus helicity injection rate calculations lack a point of reference



Welsch et al., (2007)

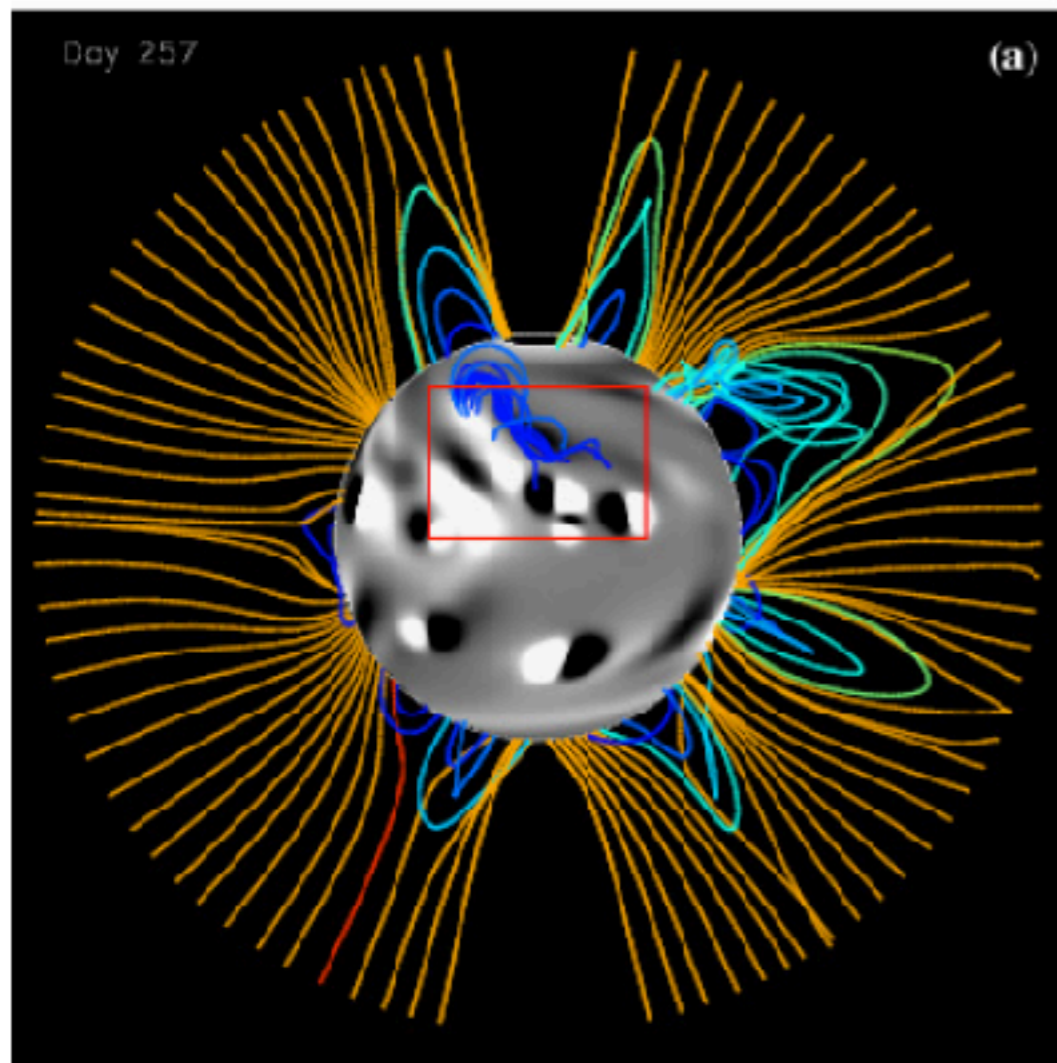


Nindos, Zhang & Zhang, (2003)

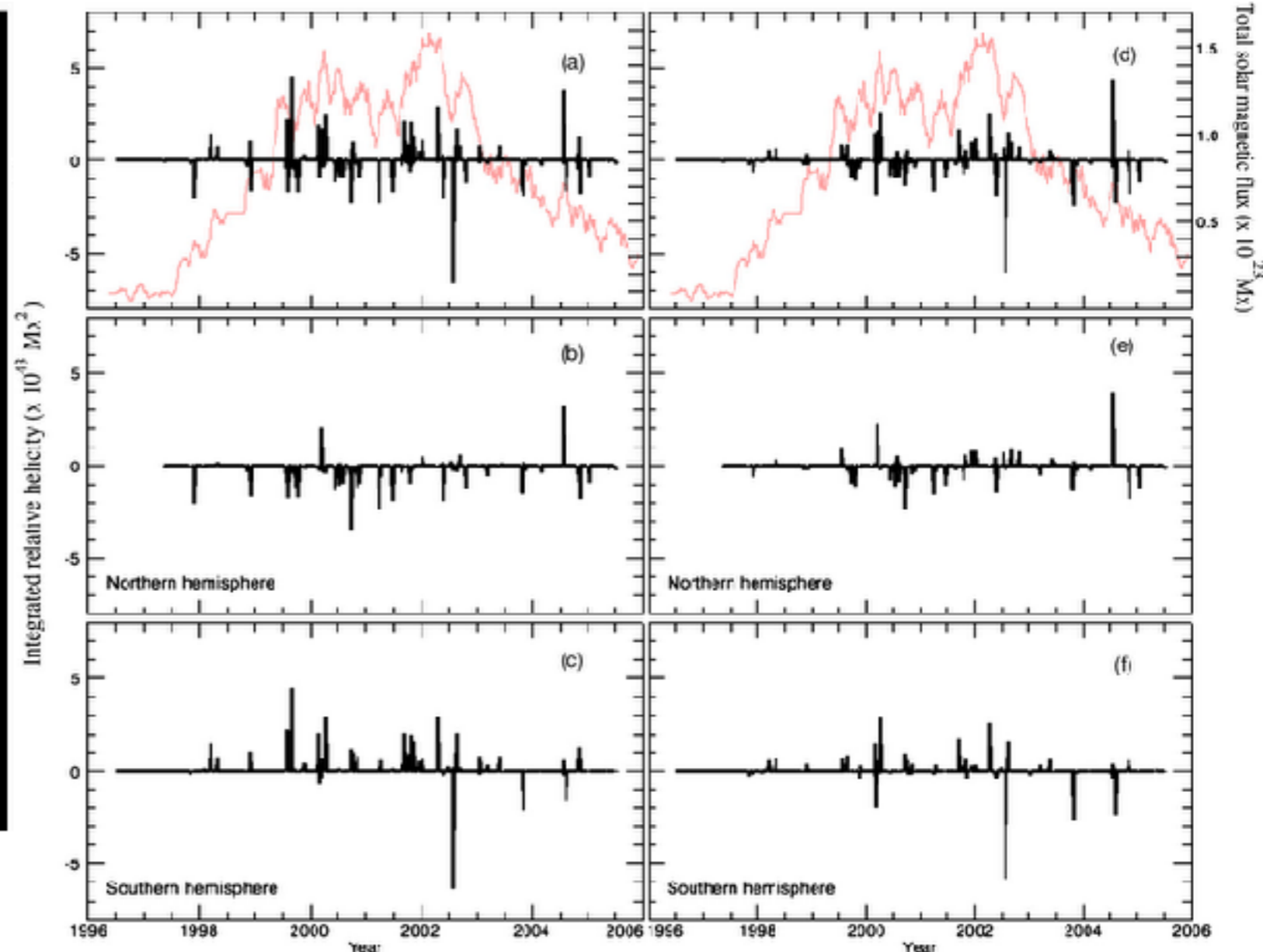
Helicity Between Global and Local Solar Scales

- Solar magnetic helicity is a global quantity, but is mostly contributed by local (i.e., active region) scales

Georgoulis et al., (2009)



Yeates et al., (2008)



- 80% of helicity stems from peculiar active-region flows; the rest from solar differential rotation
- > 99% of helicity stems from active regions; the rest from the quiet Sun

How Can We Reconcile Between Scales, Uncertainties, Caveats and Shortcomings?

- Treat (relative) magnetic helicity self-consistently with (free) magnetic energy
- If possible, disentangle detailed knowledge of the 3D field from calculation
- Define test cases — assess similarities and differences between methods

How Can We Reconcile Between Scales, Uncertainties, Caveats and Shortcomings?

- Treat (relative) magnetic helicity self-consistently with (free) magnetic energy
- If possible, disentangle detailed knowledge of the 3D field from calculation
- Define test cases — assess similarities and differences between methods

LFF field approach

$$E = \mathcal{R}_\ell \lambda^2 \alpha^2 E_p$$

$$H = 8\pi \mathcal{R}_\ell \lambda^2 \alpha E_p$$

$$H = \frac{8\pi}{\alpha} E$$

$\alpha = \text{const.}$; $\lambda \rightarrow$ length element

$$\mathcal{R}_\ell = \frac{1}{2} \sum_{l=1}^{n_x} \frac{\sum_{m=1}^{n_y} |b_{u_l;v_m}^2| / (u_l^2 + v_m^2)^{3/2}}{\sum_{m=1}^{n_y} |b_{u_l;v_m}^2| / (u_l^2 + v_m^2)^{3/2}}$$

Georgoulis & LaBonte (2007)

How Can We Reconcile Between Scales, Uncertainties, Caveats and Shortcomings?

- Treat (relative) magnetic helicity self-consistently with (free) magnetic energy
- If possible, disentangle detailed knowledge of the 3D field from calculation
- Define test cases — assess similarities and differences between methods

LFF field approach

$$E = \mathcal{R}_\ell \lambda^2 \alpha^2 E_p$$

$$H = 8\pi \mathcal{R}_\ell \lambda^2 \alpha E_p$$

$$H = \frac{8\pi}{\alpha} E$$

$\alpha = \text{const.}$; $\lambda \rightarrow$ length element

$$\mathcal{R}_\ell = \frac{1}{2} \sum_{l=1}^{n_x} \frac{\sum_{m=1}^{n_y} |b_{u_l;v_m}^2| / (u_l^2 + v_m^2)^{3/2}}{\sum_{m=1}^{n_y} |b_{u_l;v_m}^2| / (u_l^2 + v_m^2)^{3/2}}$$

NLFF field approach

$$E = \lambda^2 A \sum_{l=1}^N \alpha_l^2 \Phi_l^{2\delta} + \frac{1}{8\pi} \sum_{l=1}^N \sum_{m=1, l \neq m}^N \alpha_l \mathcal{L}_{lm}^{arch} \Phi_l \Phi_m$$

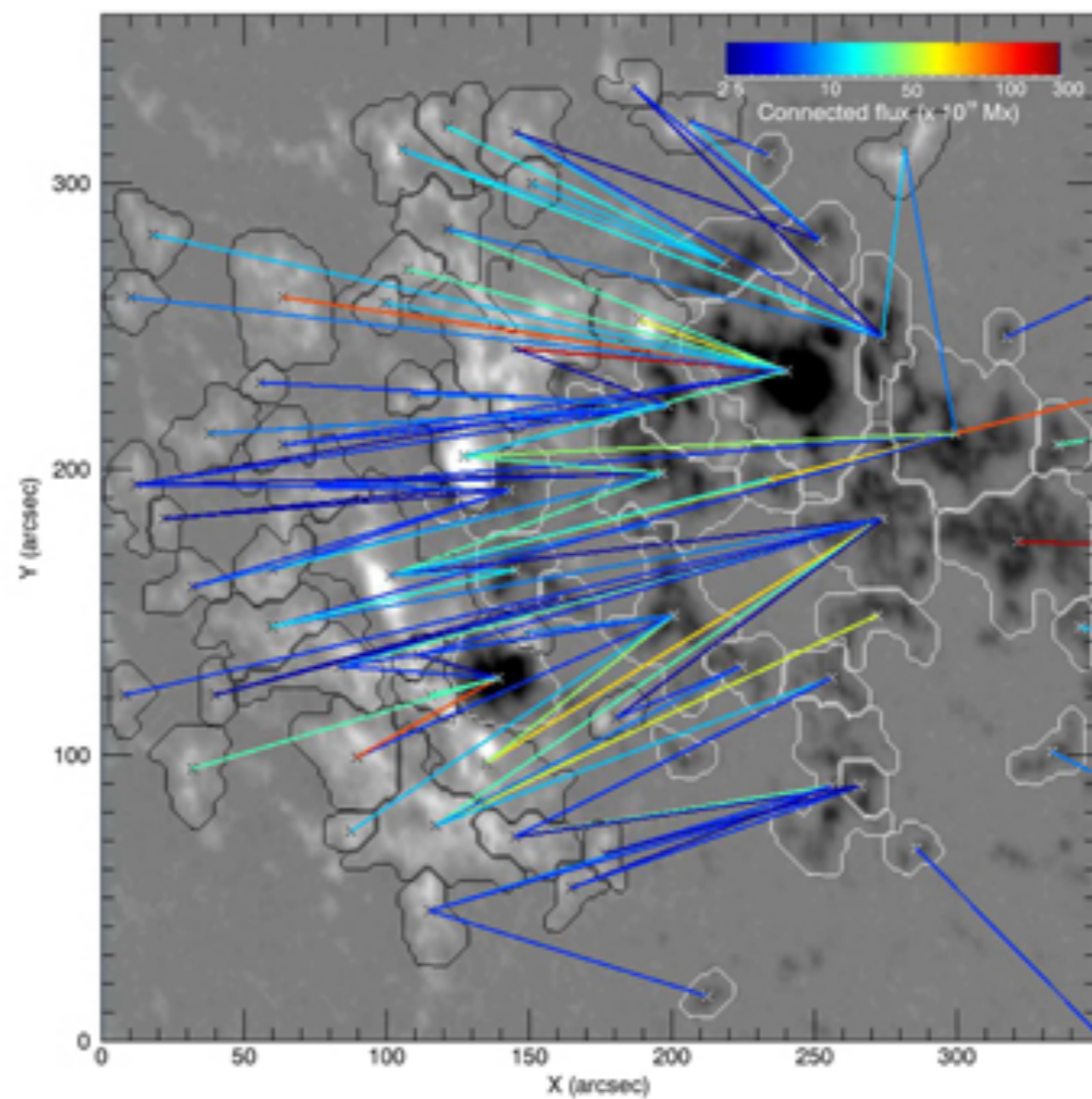
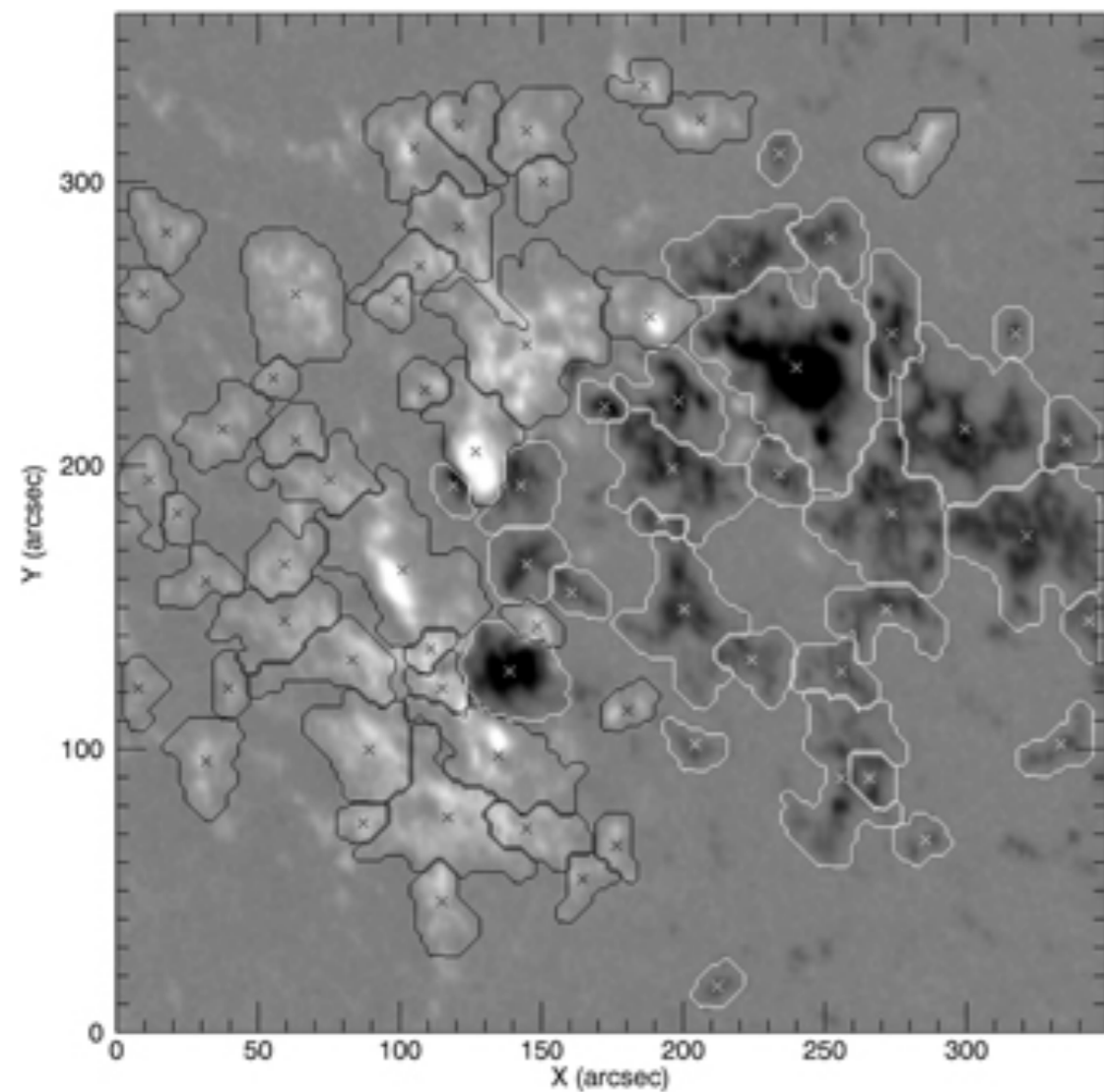
$$H = 8\pi \lambda^2 A \sum_{l=1}^N \alpha_l \Phi_l^{2\delta} + \sum_{l=1}^N \sum_{m=1, l \neq m}^N \mathcal{L}_{lm}^{arch} \Phi_l \Phi_m$$

- N flux tubes ; $\lambda \rightarrow$ length element; A, δ const.
- E is a lower limit free energy for a given connectivity that ignores intertwining of flux tubes in the corona (based on the analysis of Demoulin et al., (2006))

Georgoulis & LaBonte (2007)

Georgoulis et al., (2012)

Assessment of a Skeleton Connectivity, Without a Detailed 3D Knowledge of the Magnetic Field

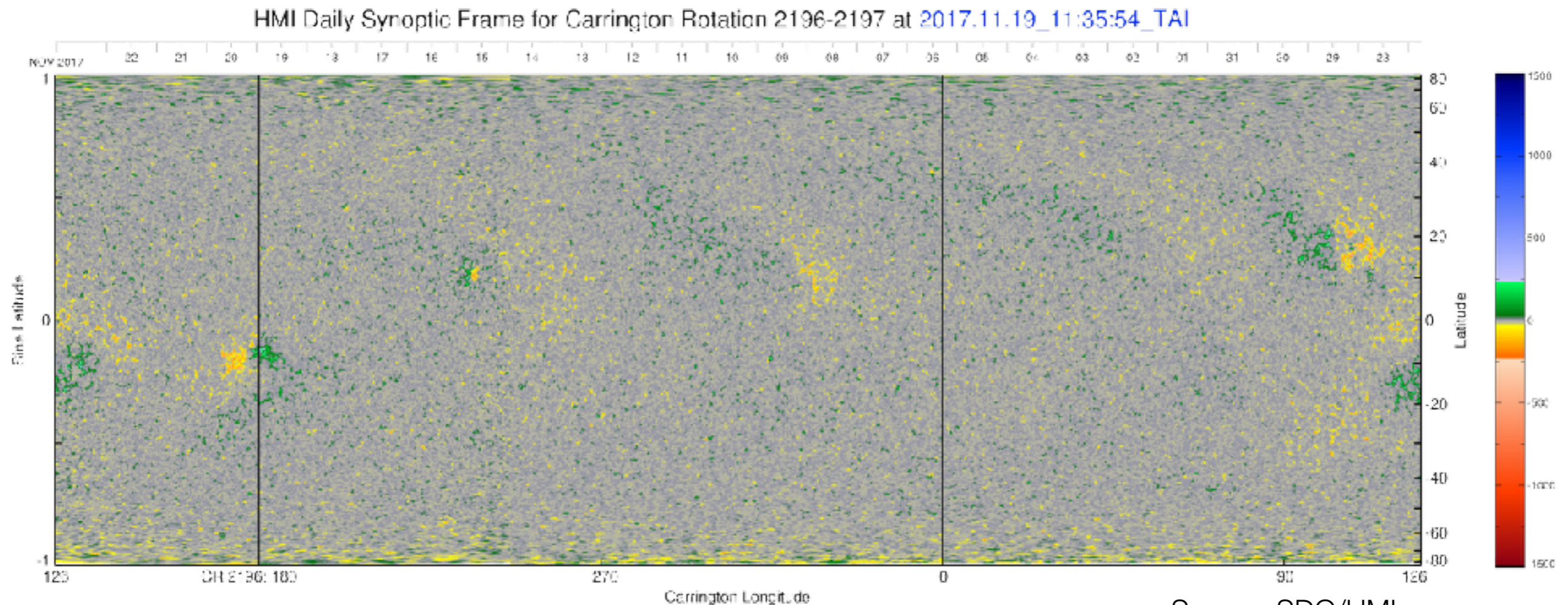


Barnes et al., (2016)

- The normal photospheric field component is partitioned; each partition assumed a different flux tube
- Connectivity inferred via a simulated annealing scheme favoring shortest connections, i.e., alongside polarity inversion lines

Can This Approach be Applied to Global Scales?

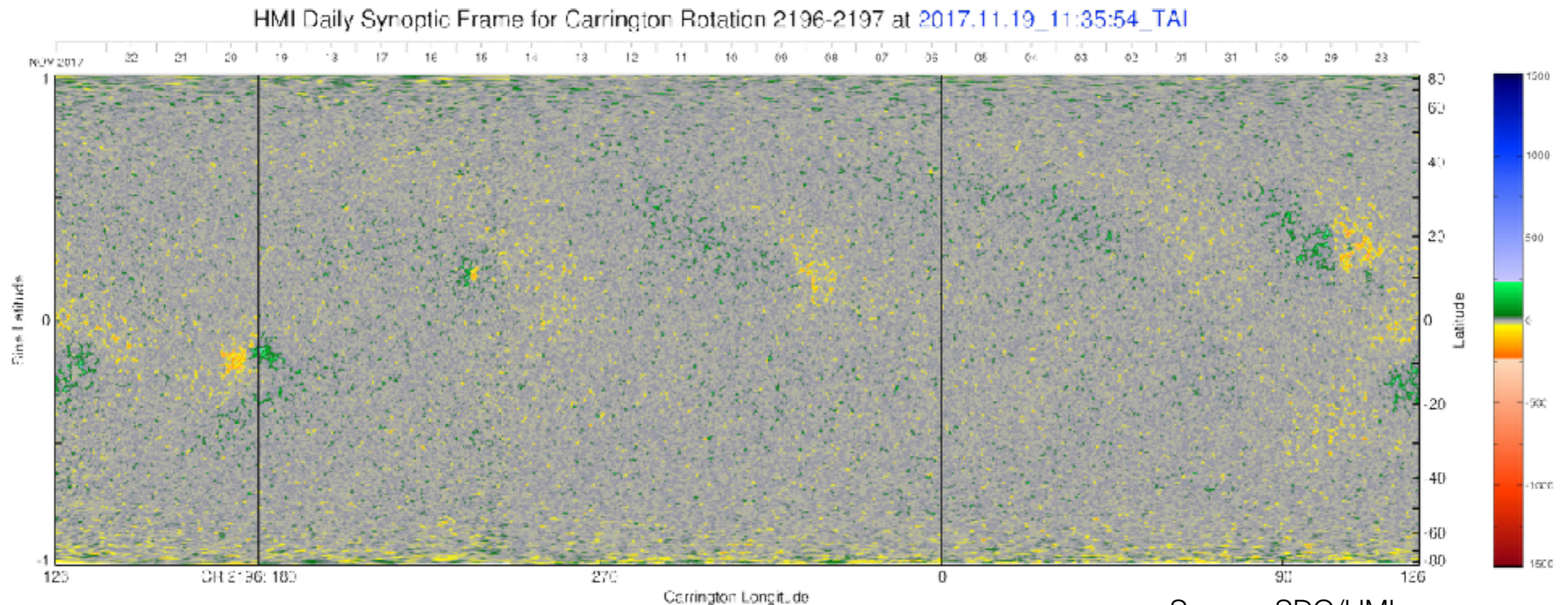
- It could, conceivably, utilizing spherical geometry on a synoptic vector magnetogram



- This scheme would find the connections within active regions first, before connecting largest scales

Can This Approach be Applied to Global Scales?

- It could, conceivably, utilizing spherical geometry on a synoptic vector magnetogram



Plot Made 10 Nov 2017 08:05:37.00

- This scheme would find the connections within active regions first, before connecting largest scales

This remains to be implemented

Testing Helicity Calculation Methods on Synthetic Test Cases

- ISSI Bern team on magnetic helicity and applications (G. Valori & E. Pariat, Team Leaders)

<p style="text-align: center;"><i>Finite volume (FV)</i></p> $\mathcal{H}_{\mathcal{V}} = \int_{\mathcal{V}} (\mathbf{A} + \mathbf{A}_p) \cdot (\mathbf{B} - \mathbf{B}_p) dV$ <p style="text-align: center;">see Eq. (3)</p> <ul style="list-style-type: none"> - Requires \mathbf{B} in \mathcal{V} e.g., from MHD simulations or NLFFF - Compute $\mathcal{H}_{\mathcal{V}}$ at one time - May employ different gauges (see Table 2) 	<p style="text-align: center;"><i>Helicity-flux integration (FI)</i></p> $\frac{d\mathcal{H}_{\mathcal{V}}}{dt} = 2 \int_{\partial\mathcal{V}} [(\mathbf{A}_p \cdot \mathbf{B})v_n - (\mathbf{A}_p \cdot \mathbf{v}_t)B_n] dS$ <ul style="list-style-type: none"> - Requires time evolution of vector field on $\partial\mathcal{V}$ - Requires knowledge or model of flows on $\partial\mathcal{V}$ - Valid for a specific set of gauge and assumptions, see Pariat et al. (2017) 		
<p style="text-align: center;"><i>Discrete flux-tubes (DT)</i></p> $\mathcal{H} \simeq \sum_{i=1}^M \mathcal{T}_i \Phi_i^2 + \sum_{i=1}^M \sum_{j=1, j \neq i}^M \mathcal{L}_{i,j} \Phi_i \Phi_j,$ <p style="text-align: center;">see Eq. (31)</p> <table style="width: 100%; border: none;"> <tr> <td style="width: 50%; vertical-align: top; padding: 5px;"> <p style="text-align: center;"><i>Twist-number (TN)</i></p> $\mathcal{H} \simeq \mathcal{T} \Phi^2$ <p style="text-align: center;">see Eq. (32)</p> <ul style="list-style-type: none"> - Estimation of the twist contribution to \mathcal{H} - Requires \mathbf{B} in \mathcal{V} - Requires a flux-rope-like structure for computing the twist \mathcal{T} </td> <td style="width: 50%; vertical-align: top; padding: 5px;"> <p style="text-align: center;"><i>Connectivity-based (CB)</i></p> $\mathcal{H} = A \sum_{i=1}^M \alpha_i \Phi_i^{2\delta} + \sum_{l,m=1}^M \mathcal{L}_{lm} \Phi_l \Phi_m$ <p style="text-align: center;">see Eq. (35)</p> <ul style="list-style-type: none"> - Requires the vector field on photosphere at one time - Models the corona connectivity as a collection of M force-free flux tubes - Minimal connection length principle </td> </tr> </table>		<p style="text-align: center;"><i>Twist-number (TN)</i></p> $\mathcal{H} \simeq \mathcal{T} \Phi^2$ <p style="text-align: center;">see Eq. (32)</p> <ul style="list-style-type: none"> - Estimation of the twist contribution to \mathcal{H} - Requires \mathbf{B} in \mathcal{V} - Requires a flux-rope-like structure for computing the twist \mathcal{T} 	<p style="text-align: center;"><i>Connectivity-based (CB)</i></p> $\mathcal{H} = A \sum_{i=1}^M \alpha_i \Phi_i^{2\delta} + \sum_{l,m=1}^M \mathcal{L}_{lm} \Phi_l \Phi_m$ <p style="text-align: center;">see Eq. (35)</p> <ul style="list-style-type: none"> - Requires the vector field on photosphere at one time - Models the corona connectivity as a collection of M force-free flux tubes - Minimal connection length principle
<p style="text-align: center;"><i>Twist-number (TN)</i></p> $\mathcal{H} \simeq \mathcal{T} \Phi^2$ <p style="text-align: center;">see Eq. (32)</p> <ul style="list-style-type: none"> - Estimation of the twist contribution to \mathcal{H} - Requires \mathbf{B} in \mathcal{V} - Requires a flux-rope-like structure for computing the twist \mathcal{T} 	<p style="text-align: center;"><i>Connectivity-based (CB)</i></p> $\mathcal{H} = A \sum_{i=1}^M \alpha_i \Phi_i^{2\delta} + \sum_{l,m=1}^M \mathcal{L}_{lm} \Phi_l \Phi_m$ <p style="text-align: center;">see Eq. (35)</p> <ul style="list-style-type: none"> - Requires the vector field on photosphere at one time - Models the corona connectivity as a collection of M force-free flux tubes - Minimal connection length principle 		

Valori et al., (2016)

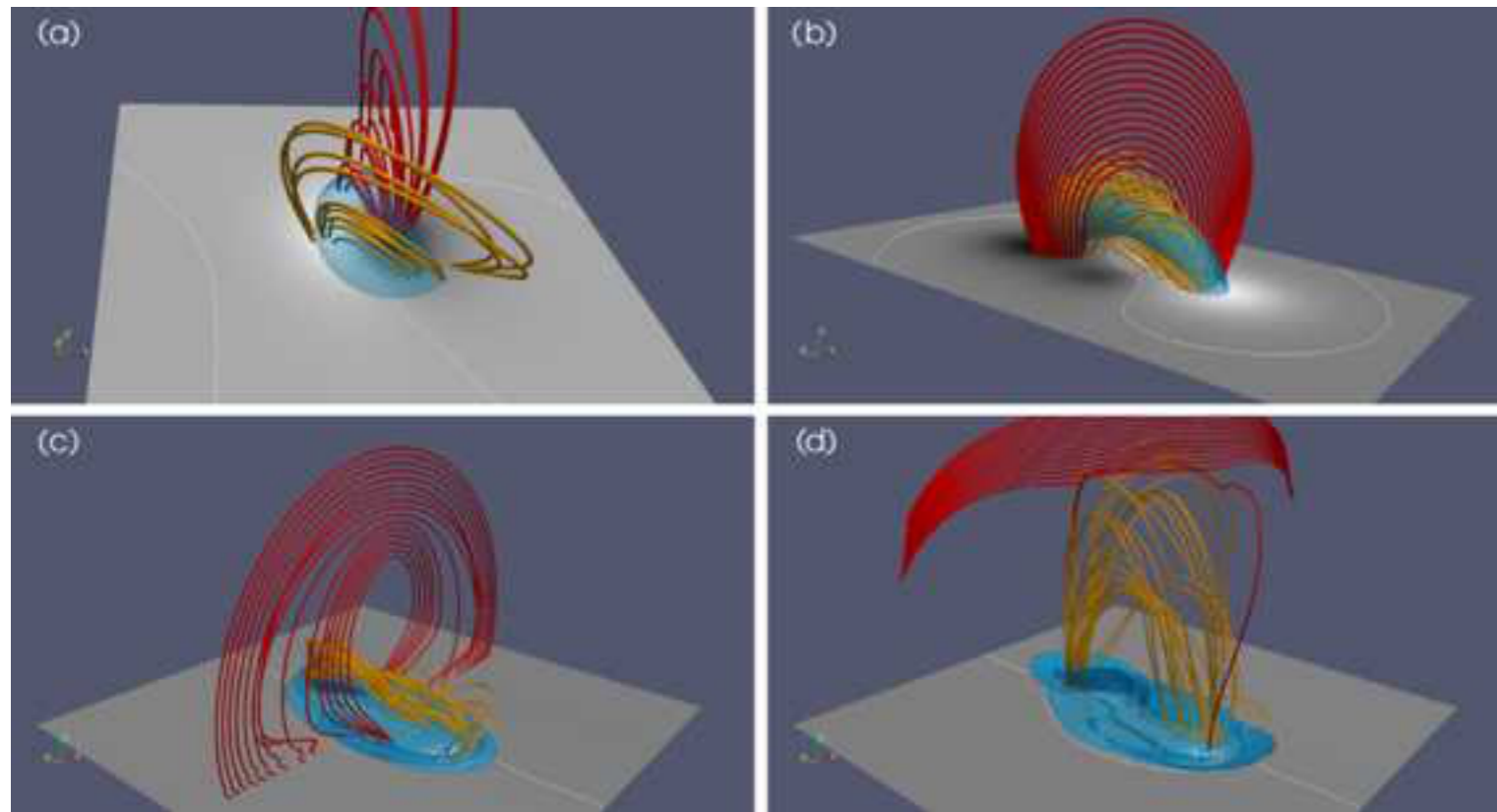
Testing Helicity Calculation Methods on Synthetic Test Cases

- ISSI Bern team on magnetic helicity and applications (G. Valori & E. Pariat, Team Leaders)

Finite volume (FV)		Helicity-flux integration (FI)				
$\mathcal{H}_{\mathcal{V}} = \int_{\mathcal{V}} (\mathbf{A} + \mathbf{A}_p) \cdot (\mathbf{B} - \mathbf{B}_p) dV$ see Eq. (3)		Method	Label	Category	Section	Reference
<ul style="list-style-type: none"> Requires \mathbf{B} in \mathcal{V} e.g., from MHD simulation NLFFF Compute $\mathcal{H}_{\mathcal{V}}$ at one time May employ different gauges (see Table 2) 		Coulomb-Thalmann	Coulomb_JT	Finite volume	Sect. 2.1.1	Thalmann et al. (2011)
		Coulomb-Yang	Coulomb_SY	Finite volume	Sect. 2.1.2	Yang et al. (2013b)
Disc $\mathcal{H} \simeq \sum_{i=1}^M \mathcal{T}_i \Phi_i^2$		Coulomb-Rudenko	Coulomb_GR	Finite volume	Sect. 2.1.3	Rudenko and Anfinogentov (2014)
Twist-number (TN) $\mathcal{H} \simeq \mathcal{T} \Phi^2$ see Eq. (32)		DeVore-Valori	DeVore_GV	Finite volume	Sect. 2.2.1	Valori et al. (2012)
<ul style="list-style-type: none"> Estimation of the twist contribution to \mathcal{H} Requires \mathbf{B} in \mathcal{V} Requires a flux-rope-like structure for computing the twist \mathcal{T} 		DeVore-Moraitis	DeVore_KM	Finite volume	Sect. 2.2.2	Moraitis et al. (2014)
		DeVore-Anfinogentov	DeVore_SA	Finite volume	Sect. 2.2.3	Not available
		Twist-number	TN	Discrete flux-tubes	Sect. 2.3.1	Guo et al. (2010)
		Connectivity-based	CB	Discrete flux-tubes	Sect. 2.3.2	Georgoulis et al. (2012)

Valori et al., (2016)

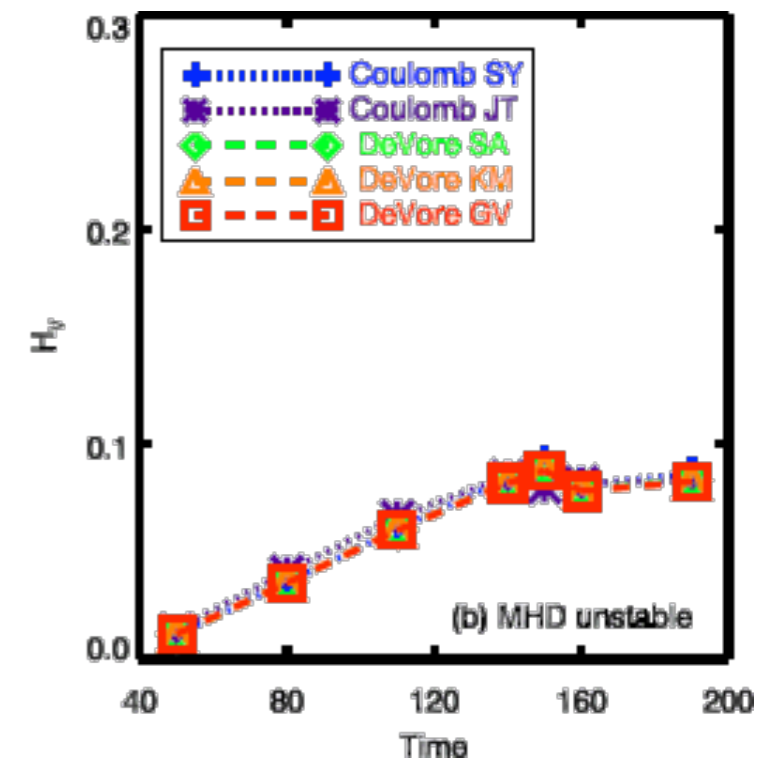
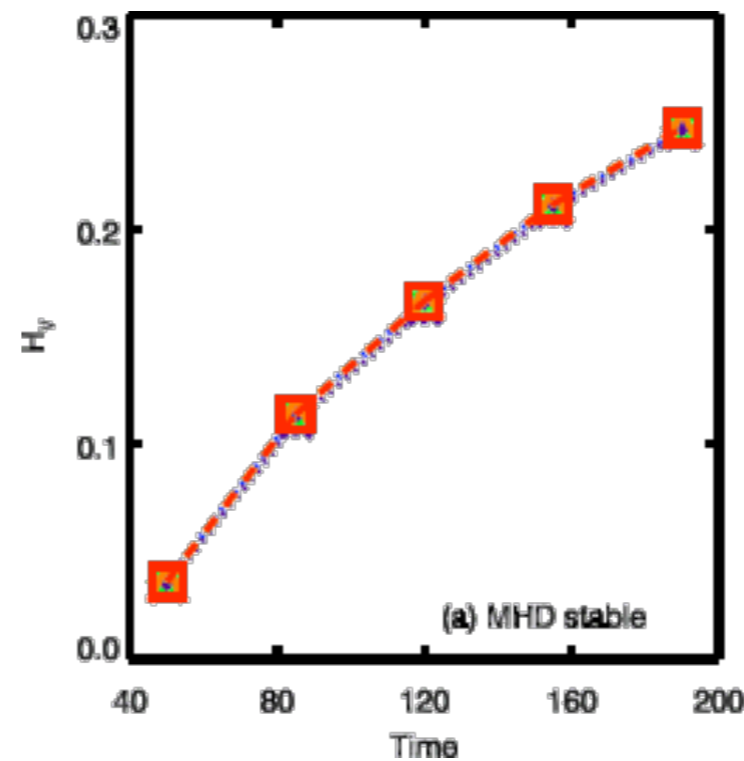
Comparison Results [1]



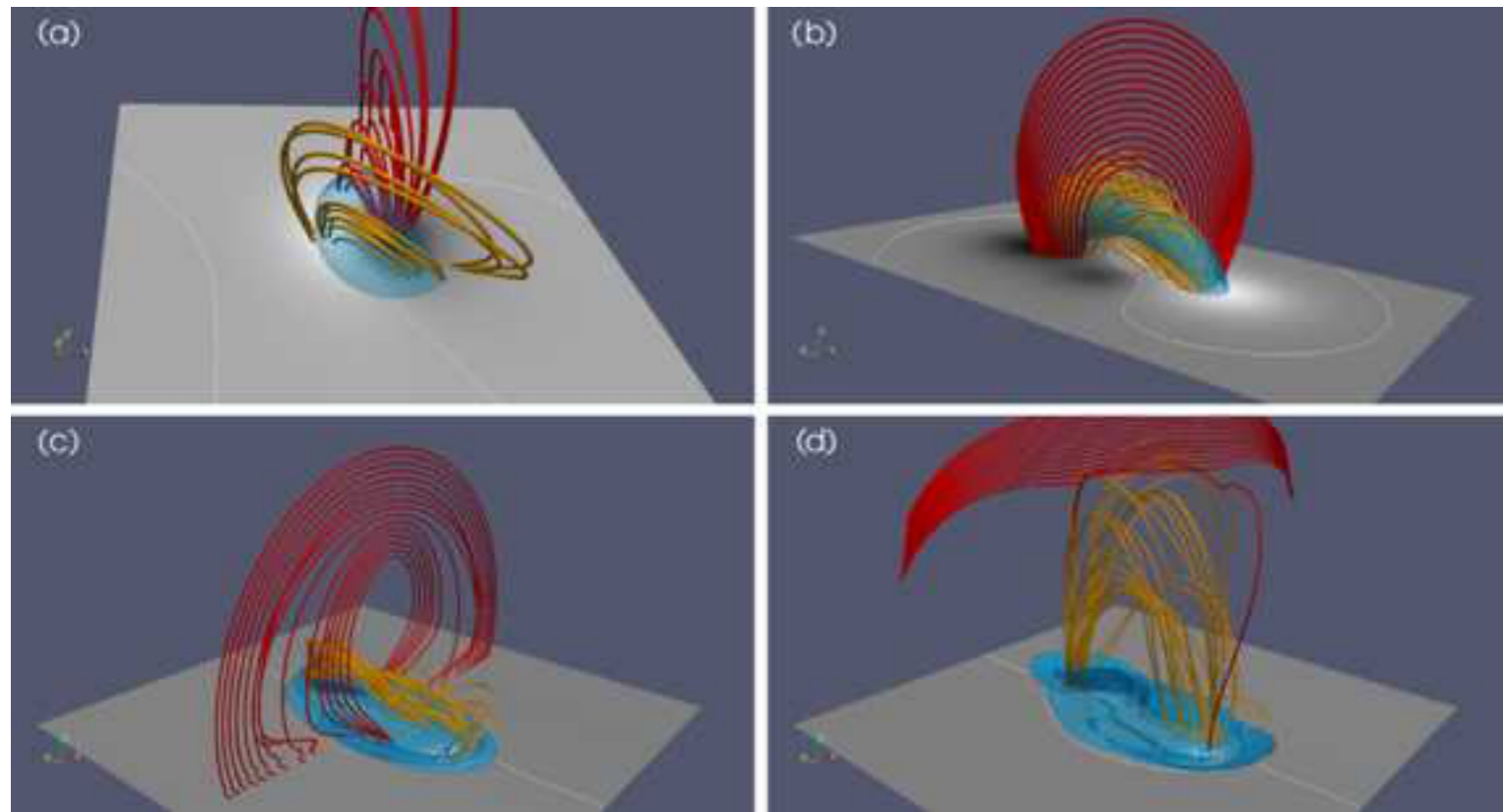
- Four selected cases
 - (a) Low & Lou FF equilibrium
 - (b) Titov & Demoulin FF equilibrium
 - (c) MHD stable model of Leake et al., (2013)
 - (d) MHD unstable model of Leake et al., (2013)

Valori et al., (2016)

- Comparison of 3D finite-volume methods in the two MHD configurations



Comparison Results [1]

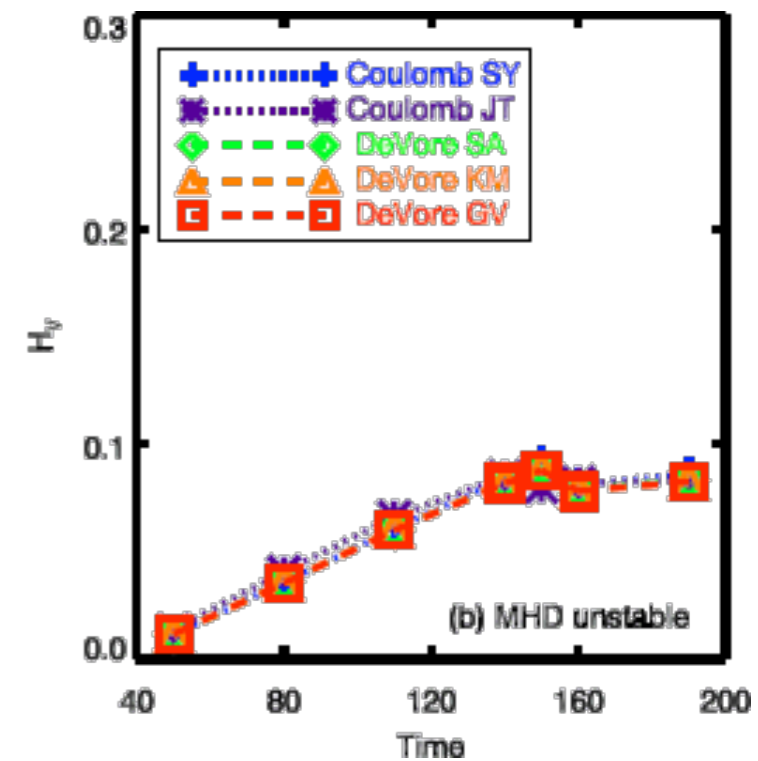
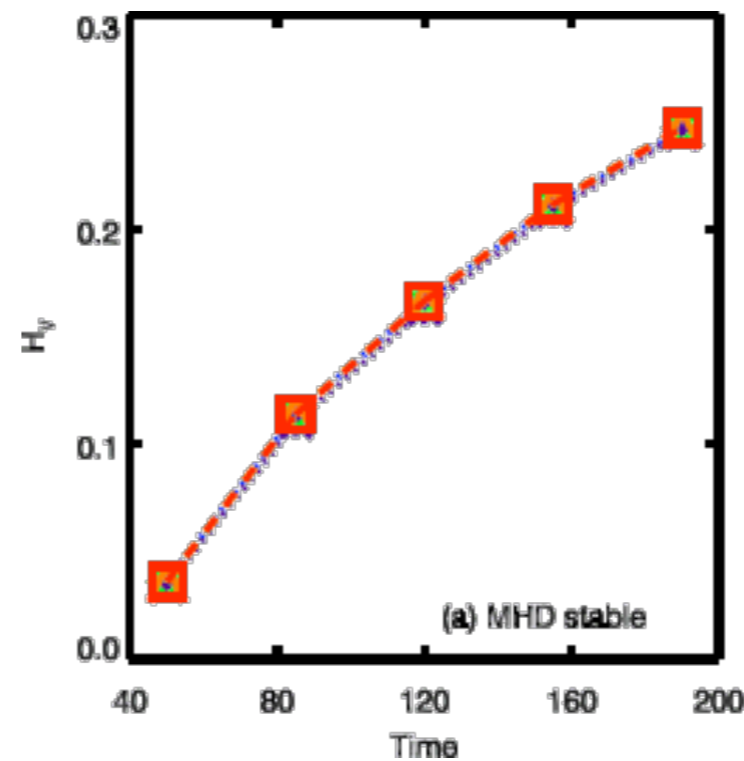


- Four selected cases
 - (a) Low & Lou FF equilibrium
 - (b) Titov & Demoulin FF equilibrium
 - (c) MHD stable model of Leake et al., (2013)
 - (d) MHD unstable model of Leake et al., (2013)

Valori et al., (2016)

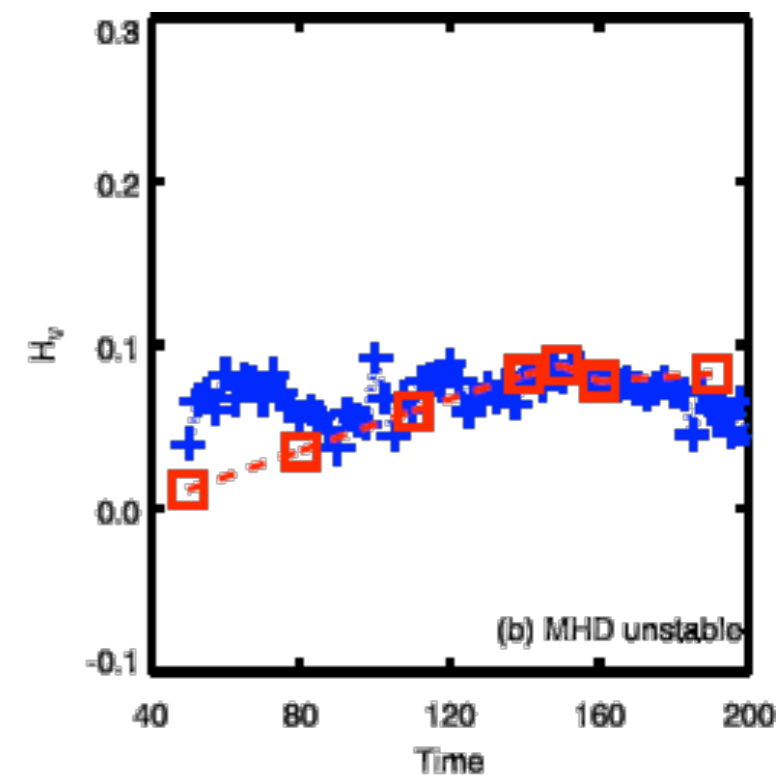
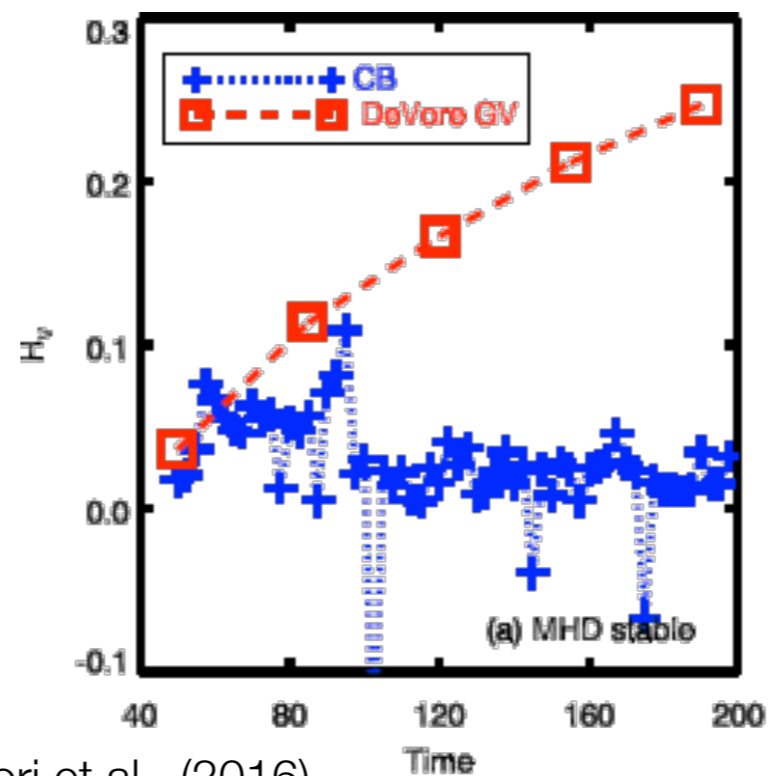
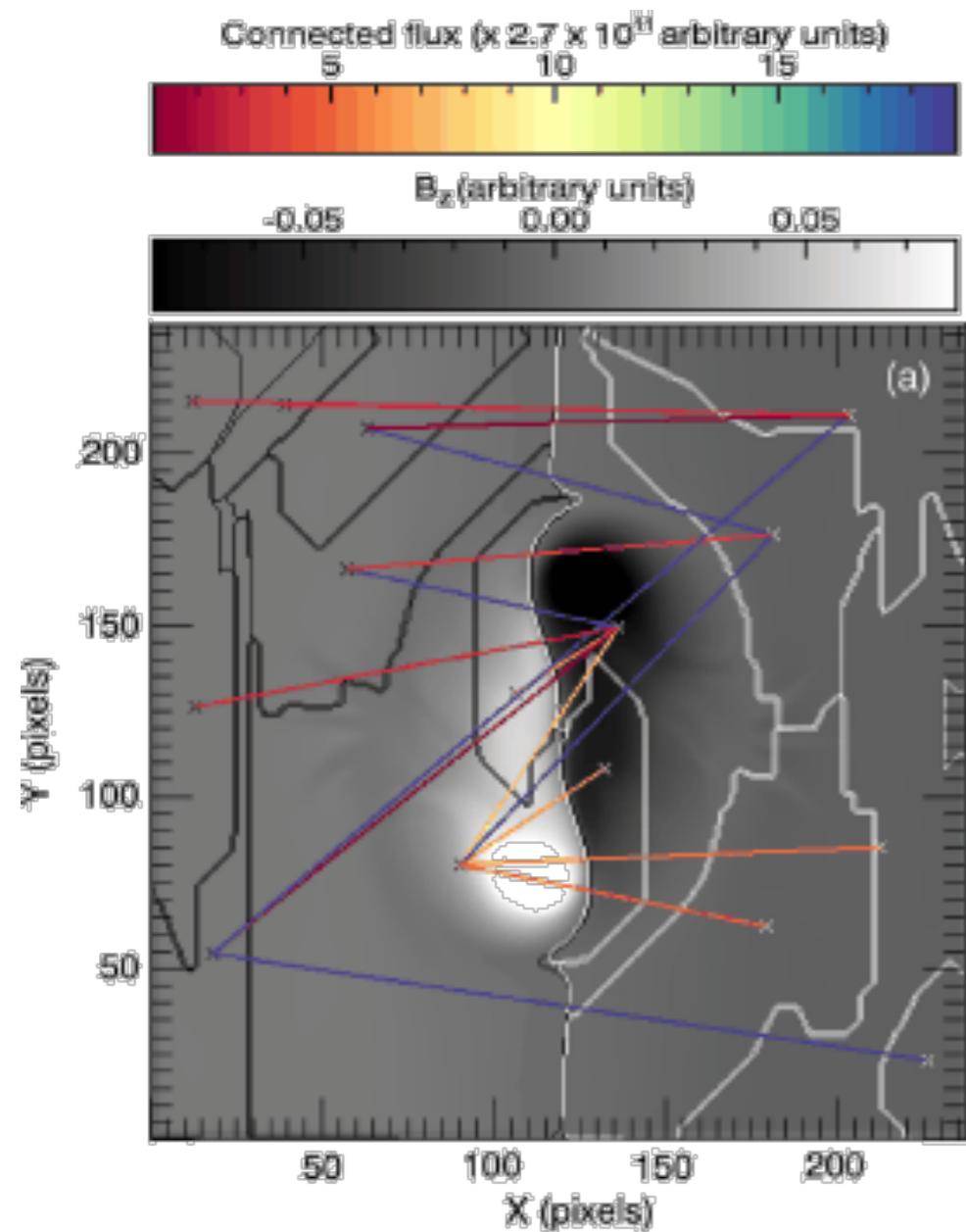
- Comparison of 3D finite-volume methods in the two MHD configurations

Pretty good agreement between methods, if 3D field is known. Also, reasonably immune results to magnetic reconnection

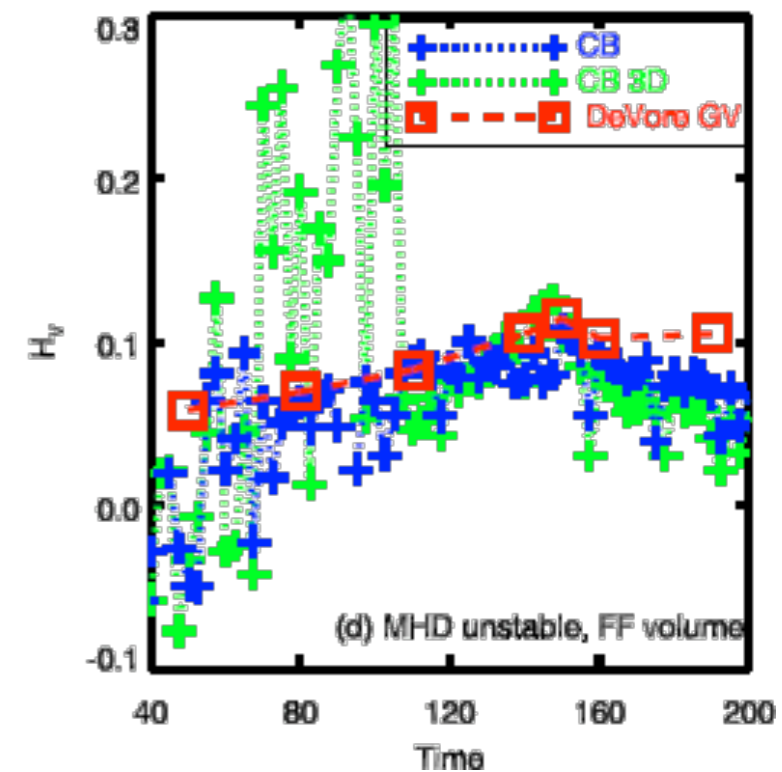
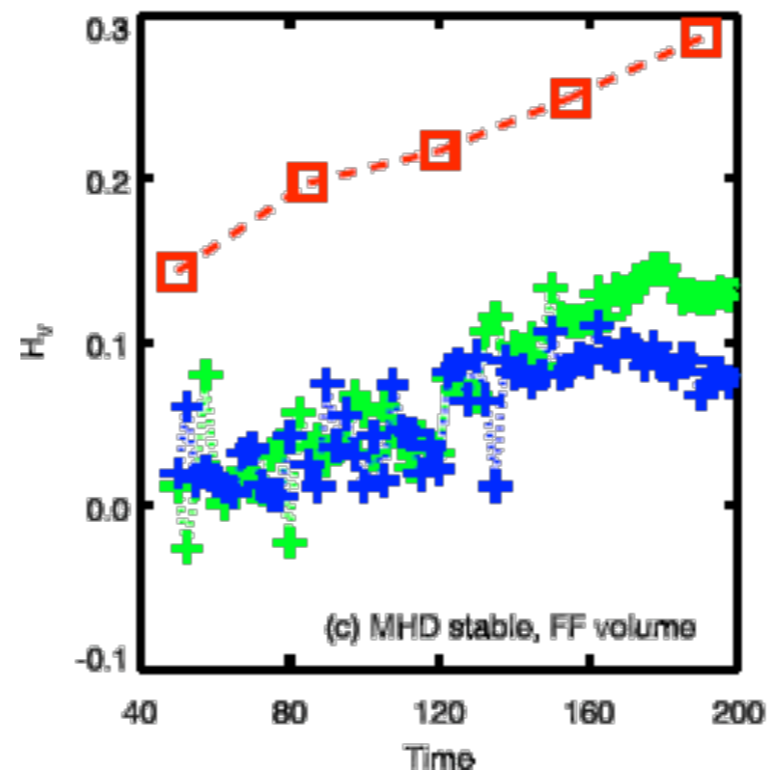


Comparison Results [2]

- Comparison between the full 3D method and the one with skeleton connectivity



Valori et al., (2016)



Less than an agreement in MHD stable configuration, but agreement within 10% for the MHD unstable one!

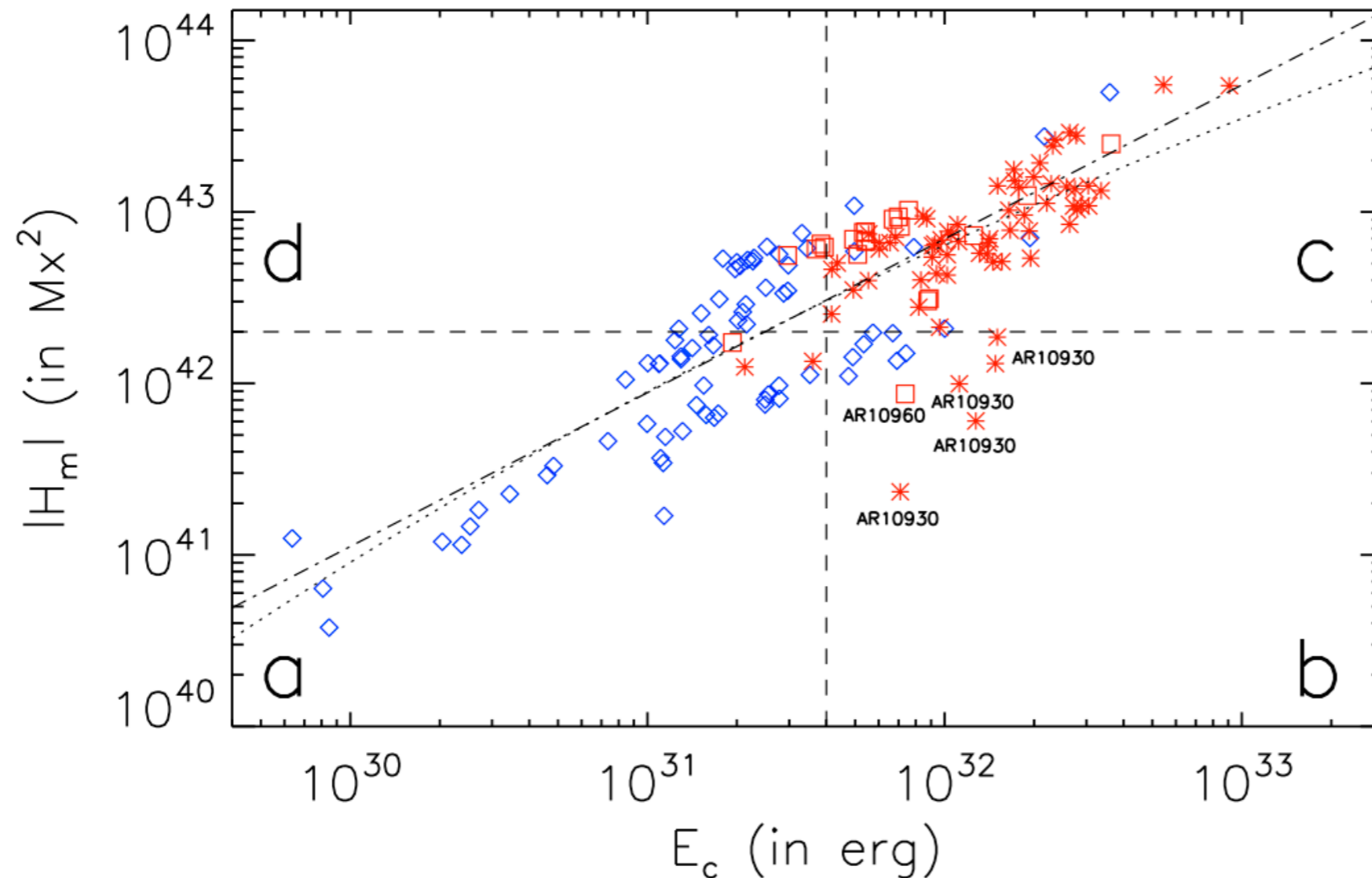
Future Steps in Correlating Magnetic Helicity

Calculation Methods

- The paper of Valori et al., (2016) is only Paper I
- In Paper II (Pariat et al., 2018, in prep.) helicity-injection rates will be tested
- In Paper III (Georgoulis et al., 2018, in prep.) methods will be tested on an NLFF-extrapolated, observed active-region case
- In another published work (Guo et al., 2017) the twist-number helicity method is applied to a number of models (Titov & Demoulin, MHD models, etc.)

Issues to Work Out. I. the “Energy — Helicity” Diagram

Tziotziou et al., 2012



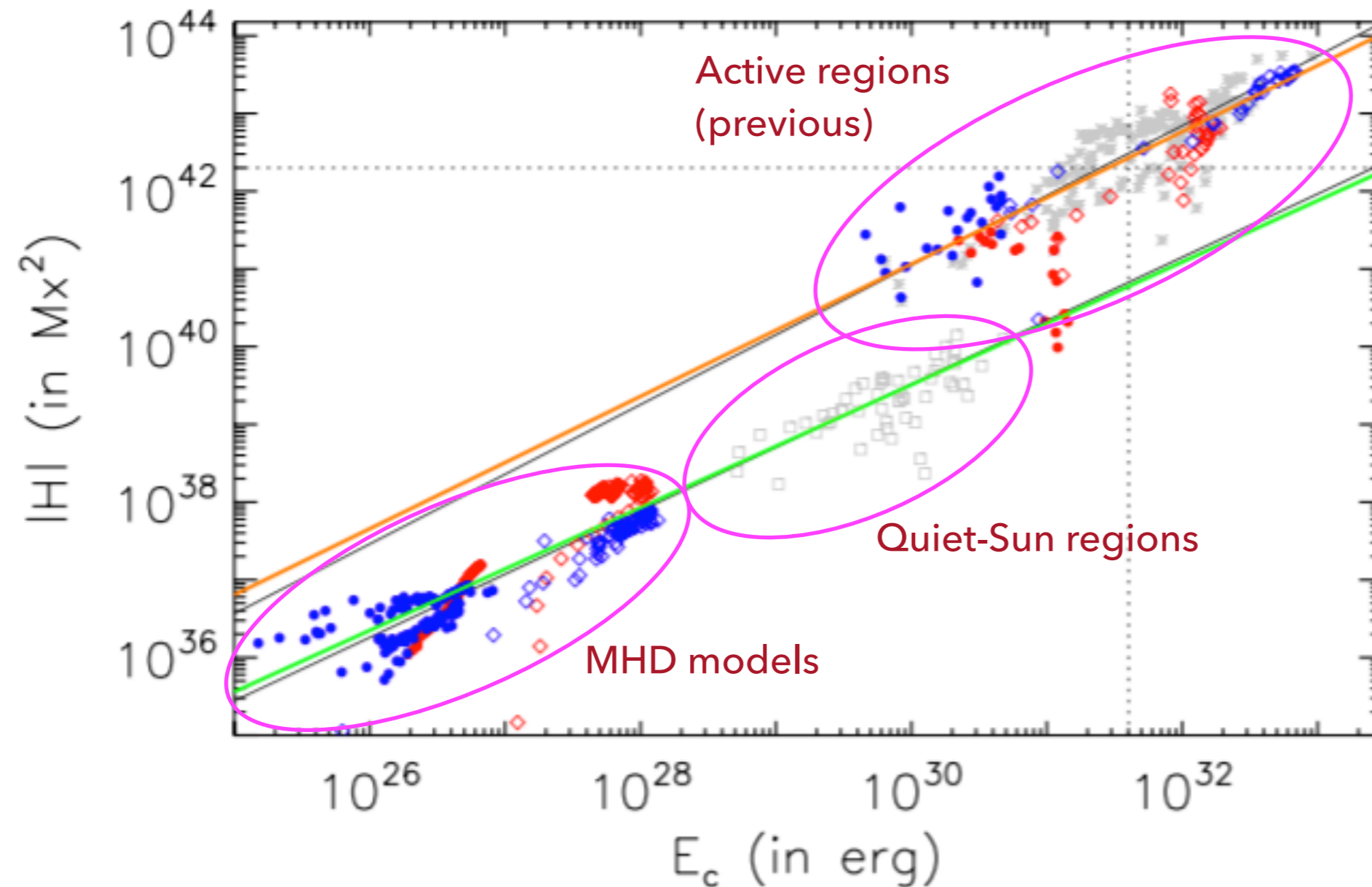
- Active regions, eruptive or not, exhibit a distinctive scaling relation between free magnetic energy and absolute value of relative magnetic helicity

$$H \propto E^{0.84 \pm 0.05}$$

- This was later noticed for quiet-Sun structures, and even for MHD models, (Tziotziou et al., 2014)

- Notice the jump to lower helicities in case of quiet-Sun structures — this points to an overall incoherence of helical sense in the quiet Sun, that might be expected, but need to be investigated further

Issues to Work Out. I. the “Energy — Helicity” Diagram



- Active regions, eruptive or not, exhibit a distinctive scaling relation between free magnetic energy and absolute value of relative magnetic helicity

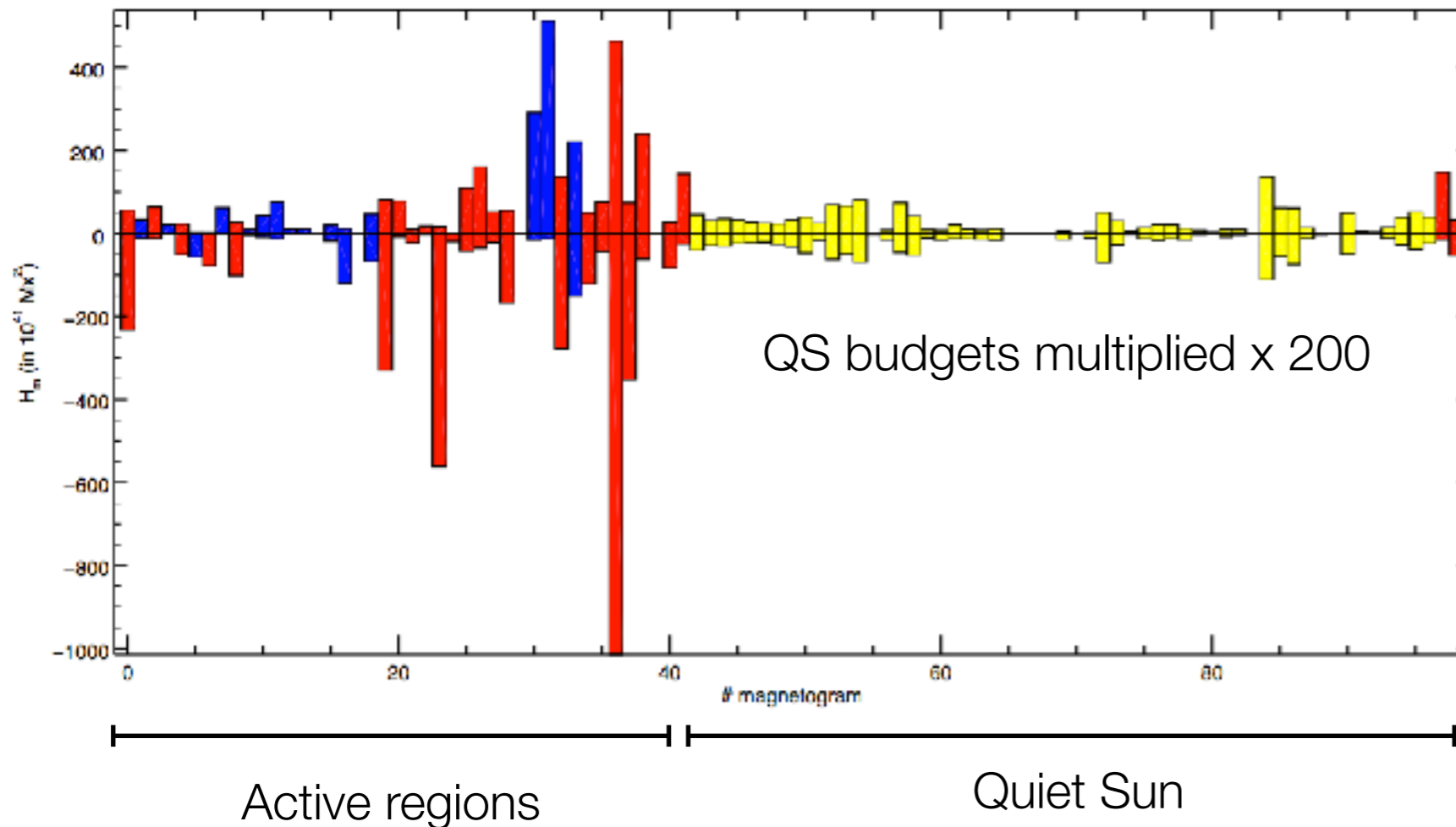
$$H \propto E^{0.84 \pm 0.05}$$

- This was later noticed for quiet-Sun structures, and even for MHD models, (Tziotziou et al., 2014)

- Notice the jump to lower helicities in case of quiet-Sun structures — this points to an overall incoherence of helical sense in the quiet Sun, that might be expected, but need to be investigated further

Issues to Work Out. II. Competition of the Two Helicity Senses

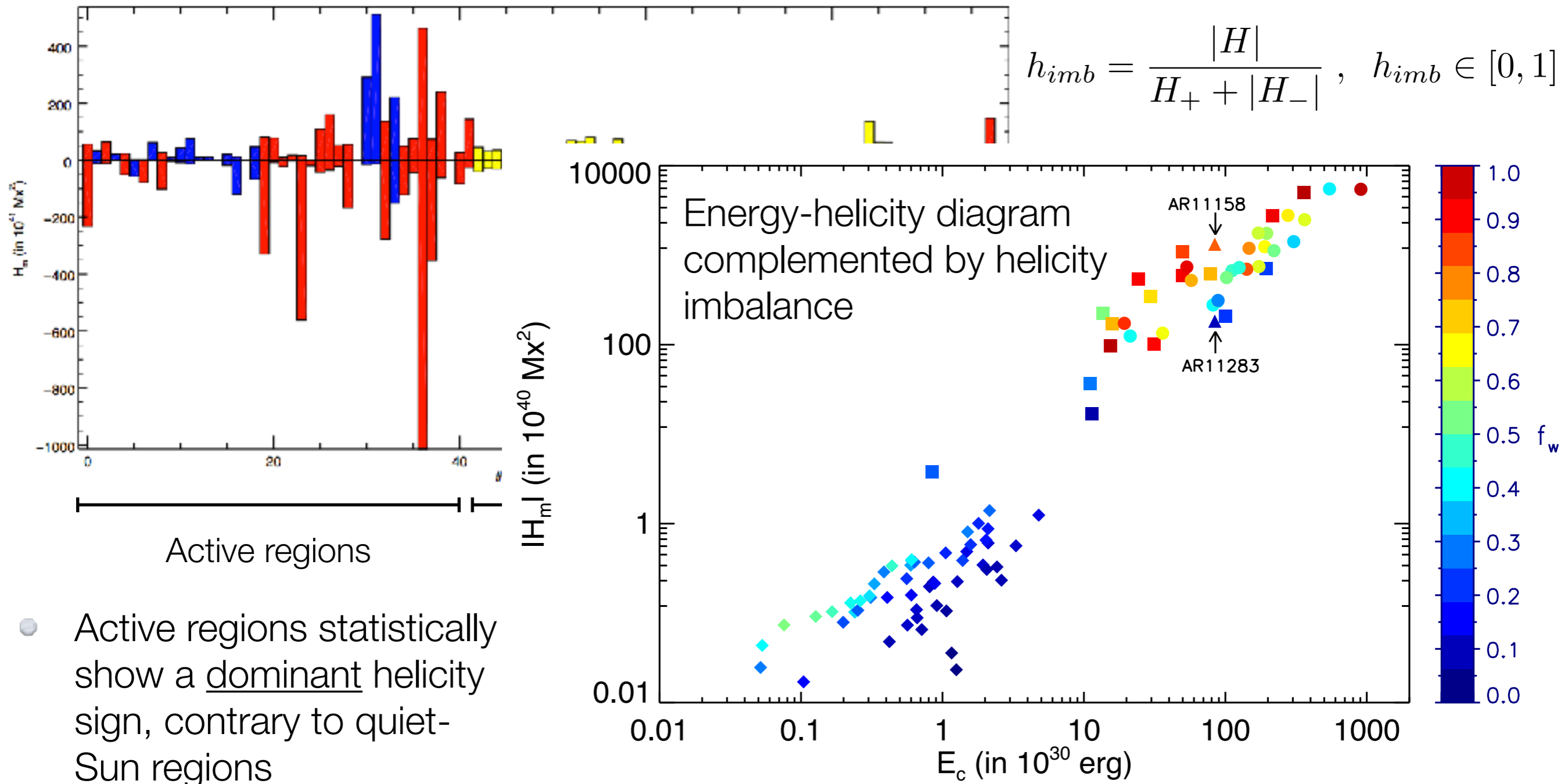
- Our discrete relative helicity calculation method enables the calculation of both signs of helicity within a given magnetic structure



- Active regions statistically show a dominant helicity sign, contrary to quiet-Sun regions

Issues to Work Out. II. Competition of the Two Helicity Senses

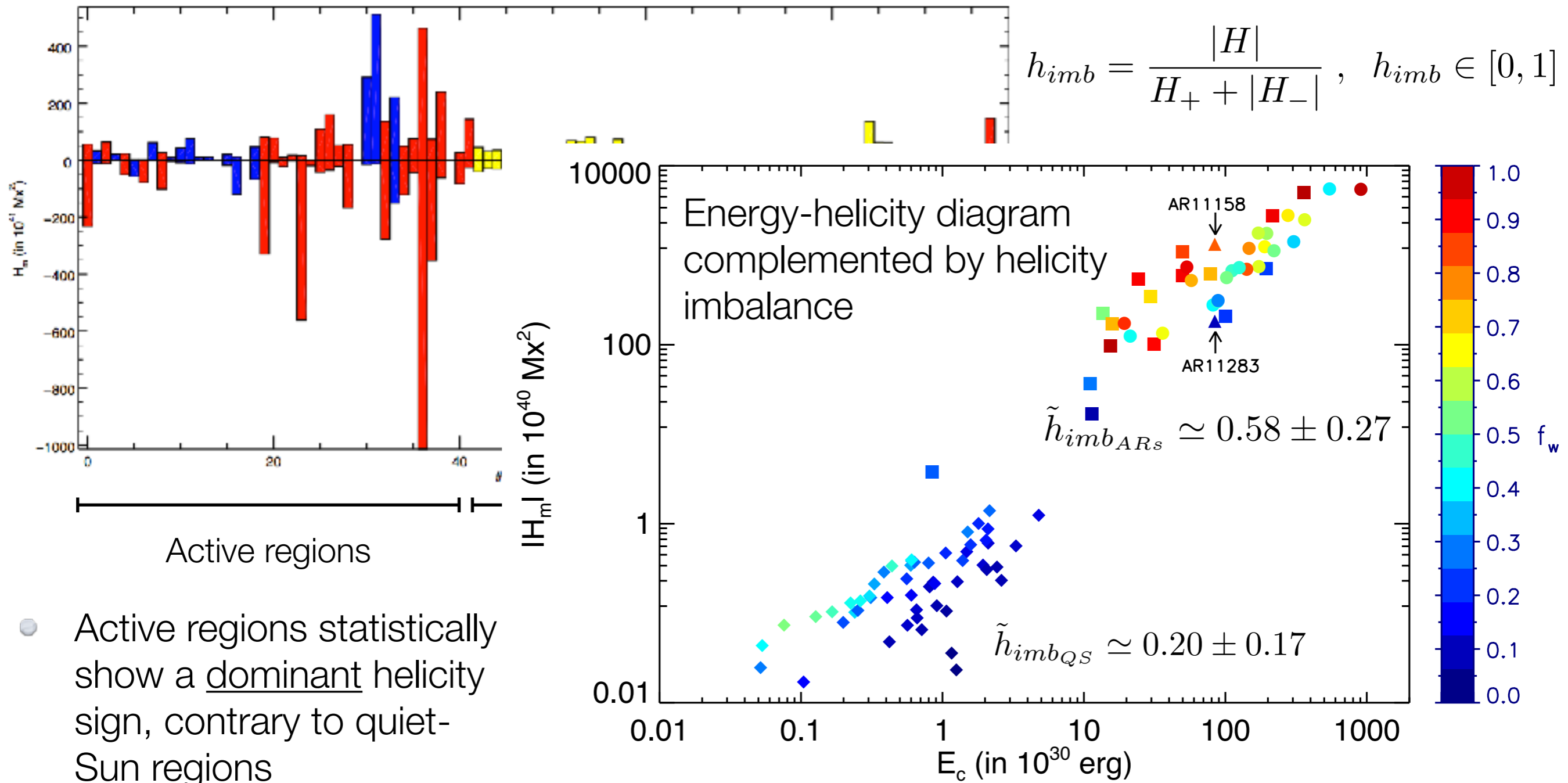
- Our discrete relative helicity calculation method enables the calculation of both signs of helicity within a given magnetic structure



- Active regions statistically show a dominant helicity sign, contrary to quiet-Sun regions

Issues to Work Out. II. Competition of the Two Helicity Senses

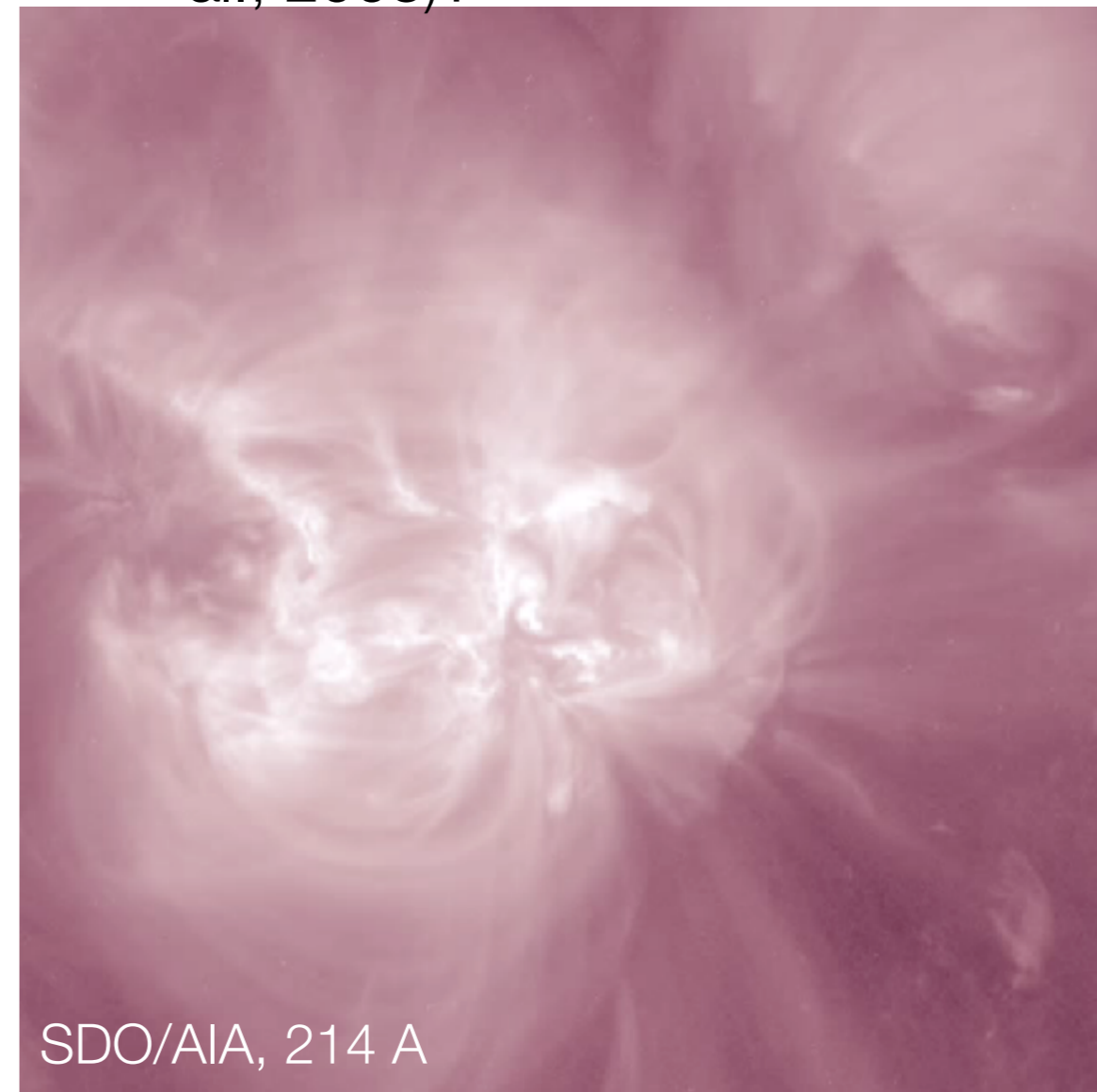
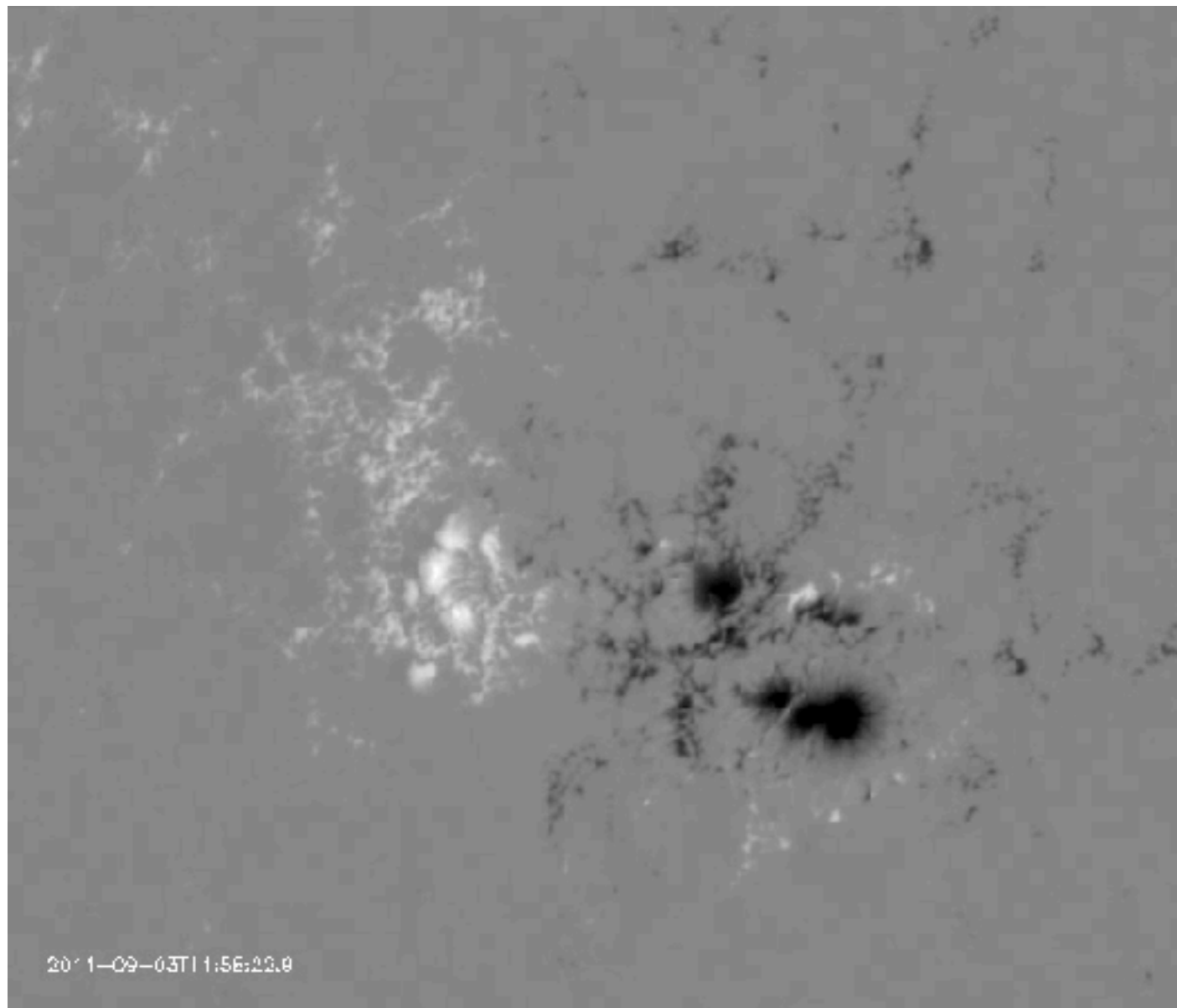
- Our discrete relative helicity calculation method enables the calculation of both signs of helicity within a given magnetic structure



- Active regions statistically show a dominant helicity sign, contrary to quiet-Sun regions

Exceptions? Of Course, Even Significant Ones

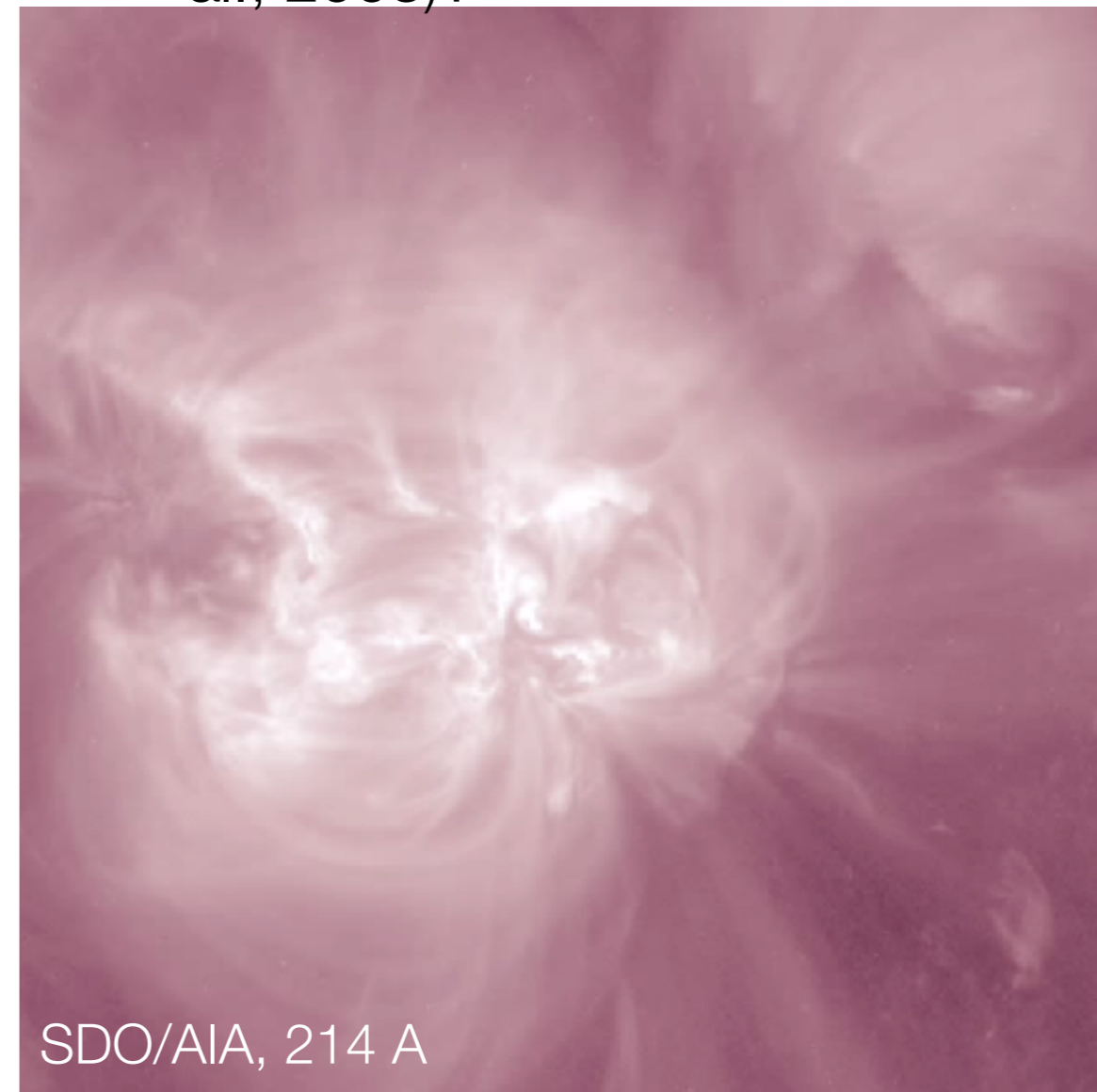
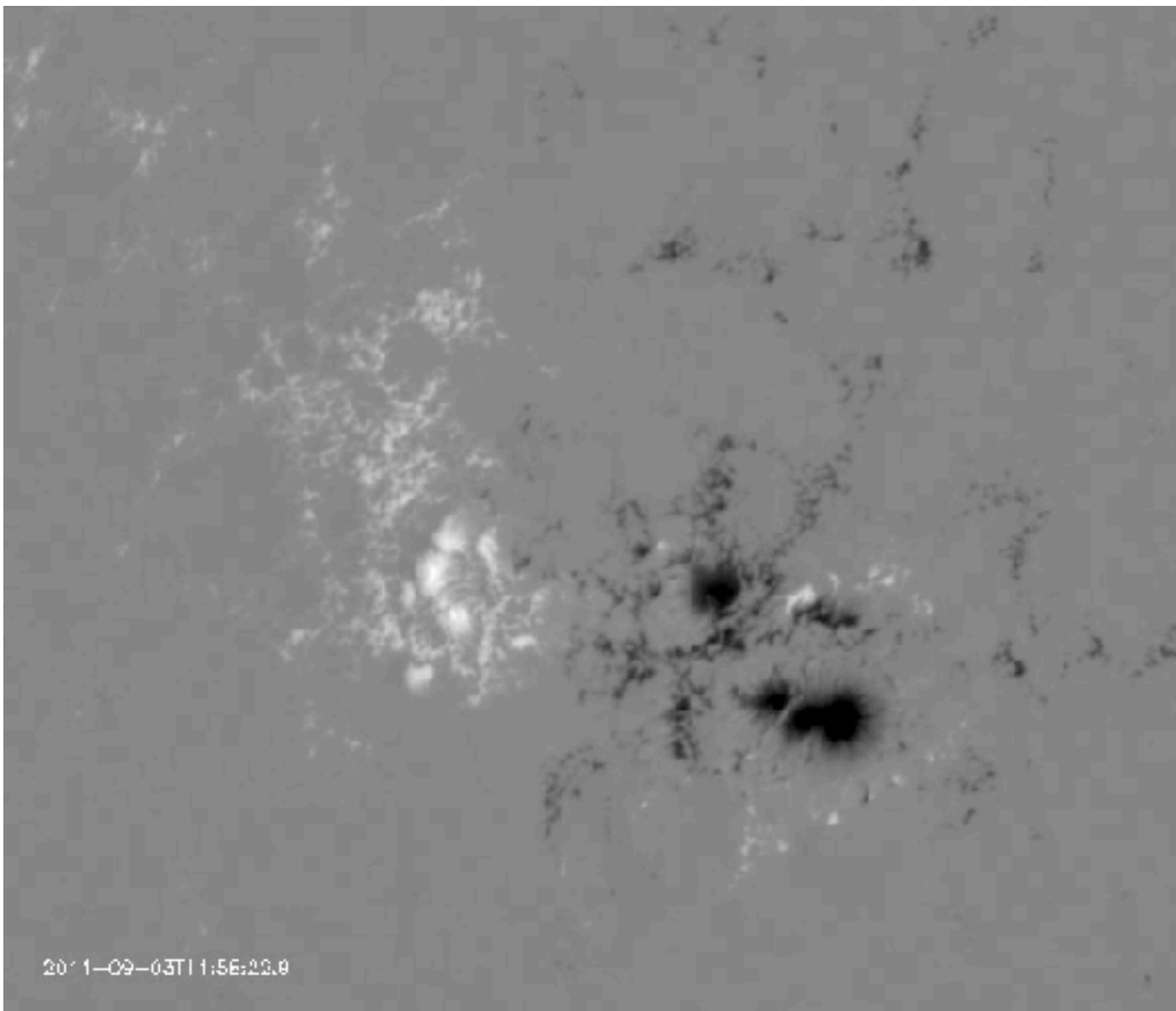
- NOAA AR 11283, on Sep 2011
- Initially left-handed configuration
- Gives two eruptive X-class flares with very low helicity
- Helicity annihilation (Kusano et al., 2003)?



- Both X-class flares relate to eruptions of right-handed structures (e.g., Jiang et al., 2013)

Exceptions? Of Course, Even Significant Ones

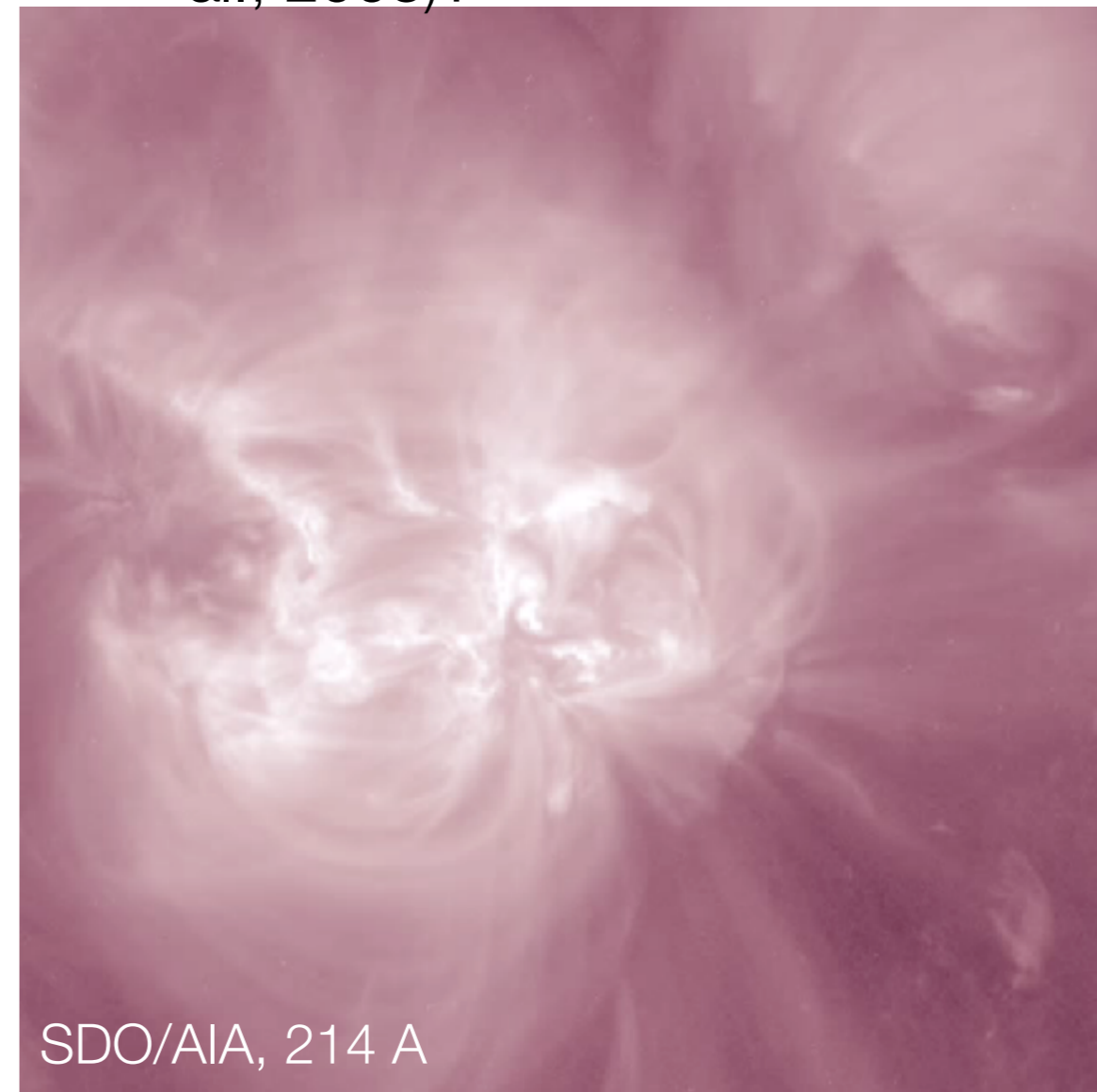
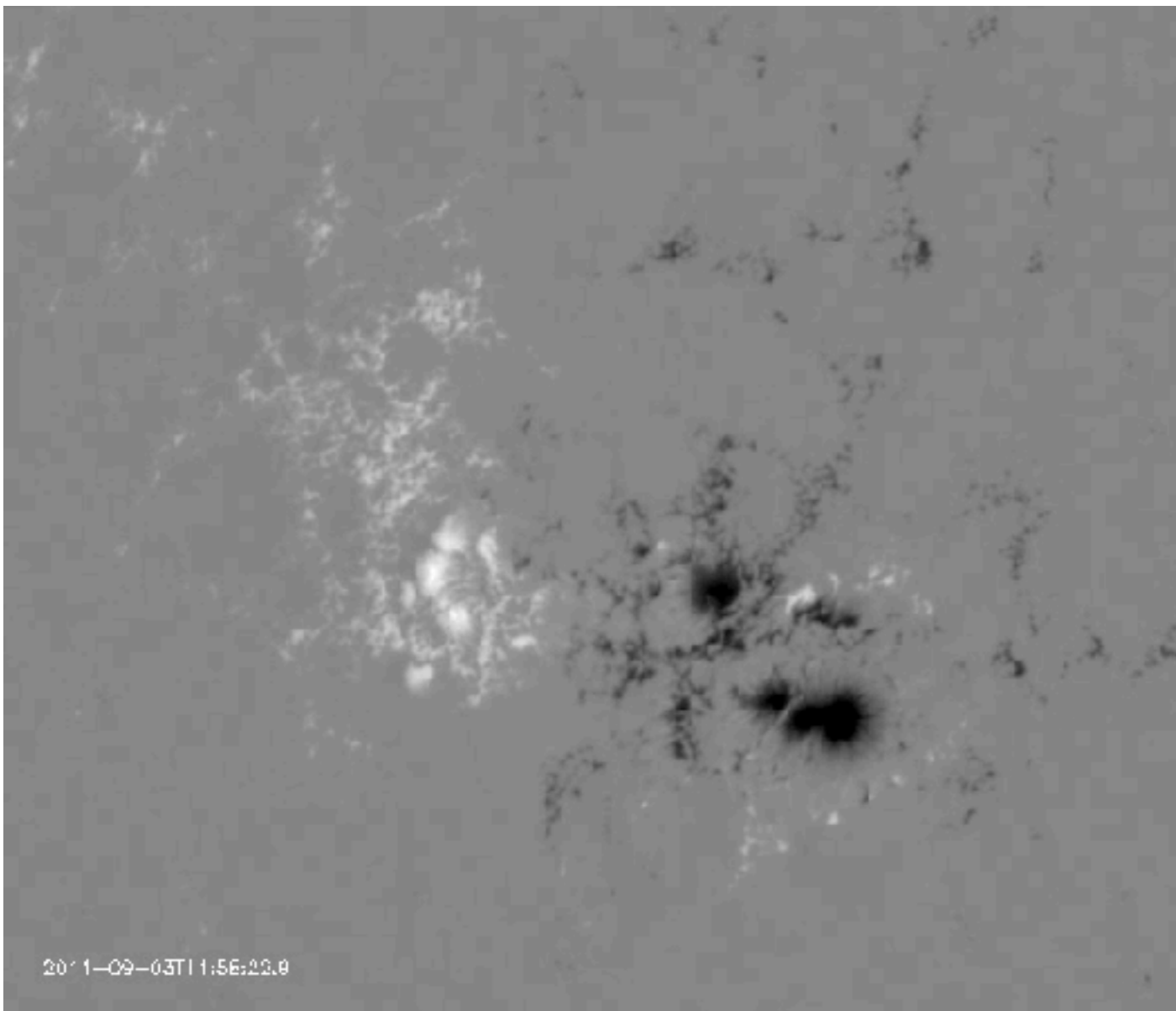
- NOAA AR 11283, on Sep 2011
- Initially left-handed configuration
- Gives two eruptive X-class flares with very low helicity
- Helicity annihilation (Kusano et al., 2003)?



- Both X-class flares relate to eruptions of right-handed structures (e.g., Jiang et al., 2013)

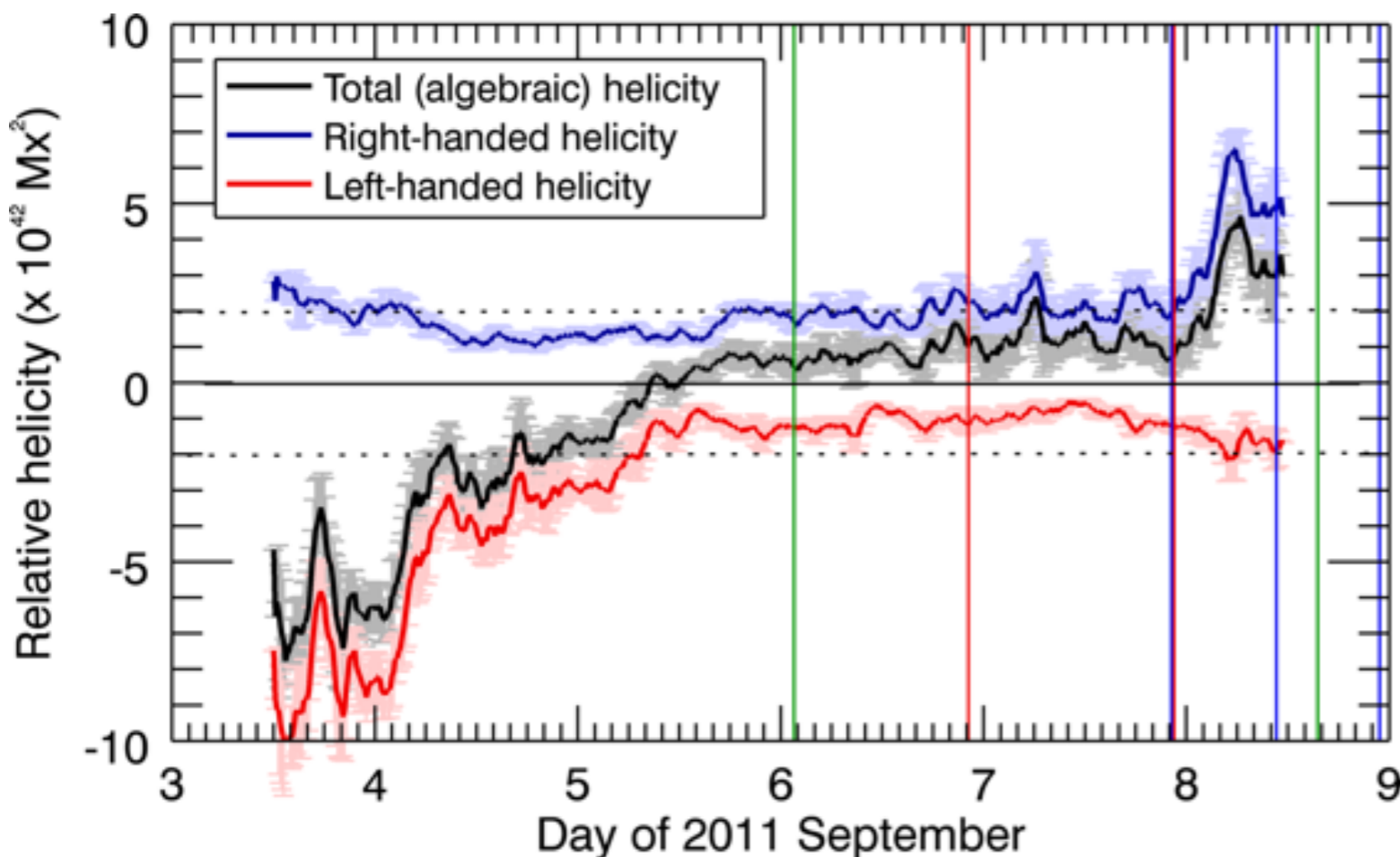
Exceptions? Of Course, Even Significant Ones

- NOAA AR 11283, on Sep 2011
- Initially left-handed configuration
- Gives two eruptive X-class flares with very low helicity
- Helicity annihilation (Kusano et al., 2003)?

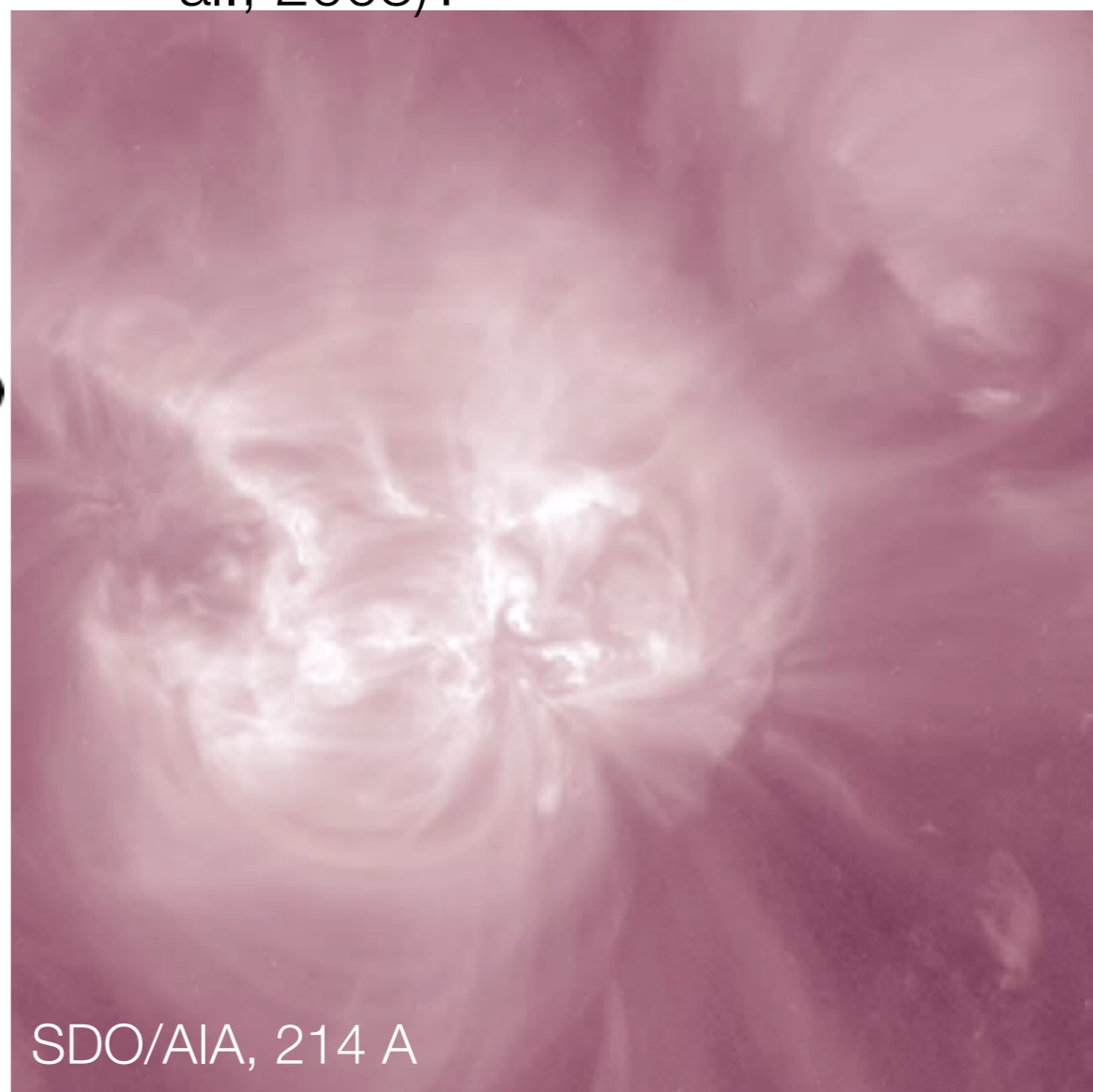


- Both X-class flares relate to eruptions of right-handed structures (e.g., Jiang et al., 2013)

Exceptions? Of Course, Even Significant Ones



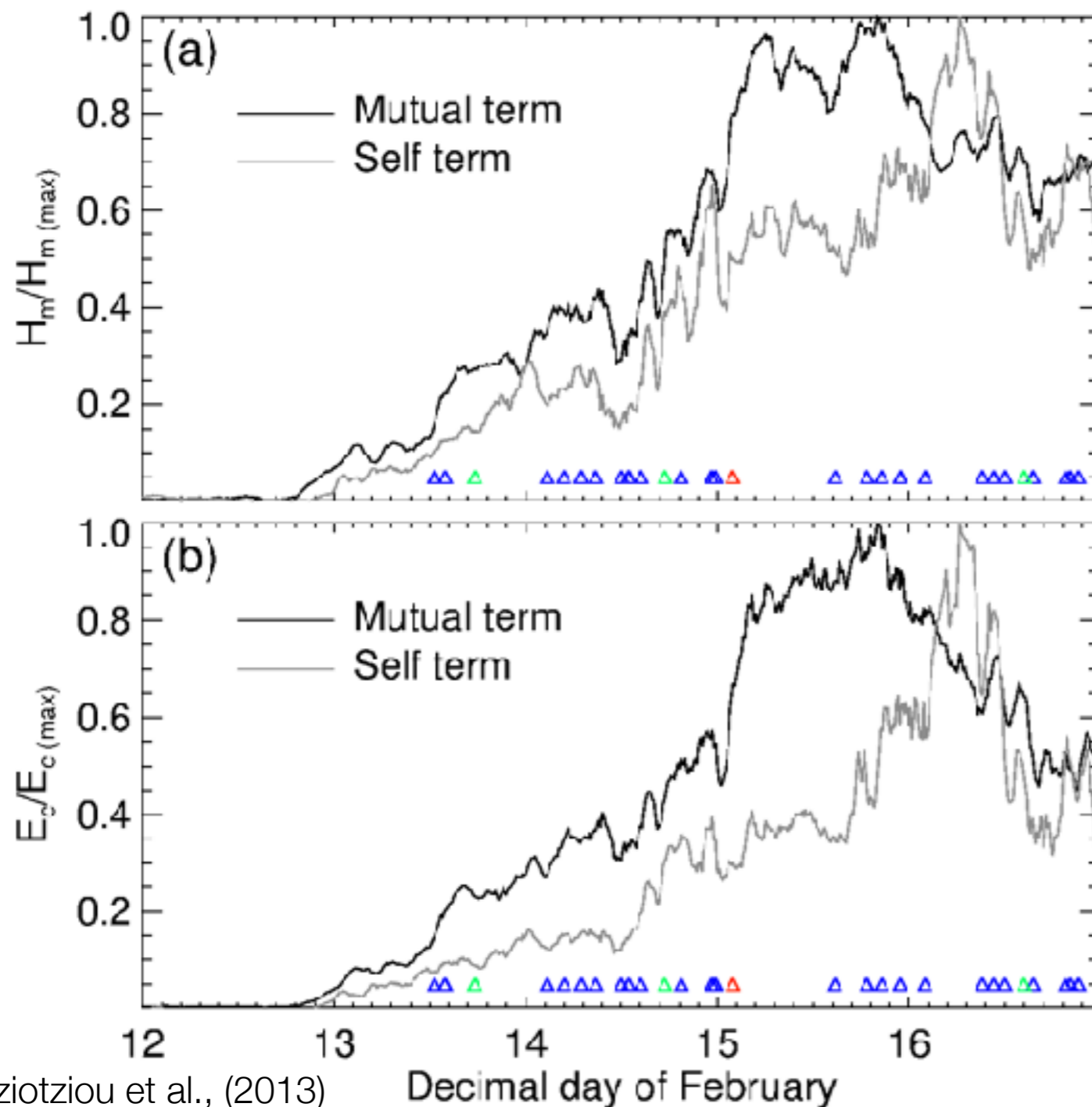
- NOAA AR 11283, on Sep 2011
- Initially left-handed configuration
- Gives two eruptive X-class flares with very low helicity
- Helicity annihilation (Kusano et al., 2003)?



- Both X-class flares relate to eruptions of right-handed structures (e.g., Jiang et al., 2013)
- What seems to happen? Initially left-handed structure gradually turns into a right-handed one

Issues to Work Out. III. Mutual vs. Self Helicity

- Our discrete relative helicity calculation method also enables separation between self and mutual terms of relative helicity and free energy

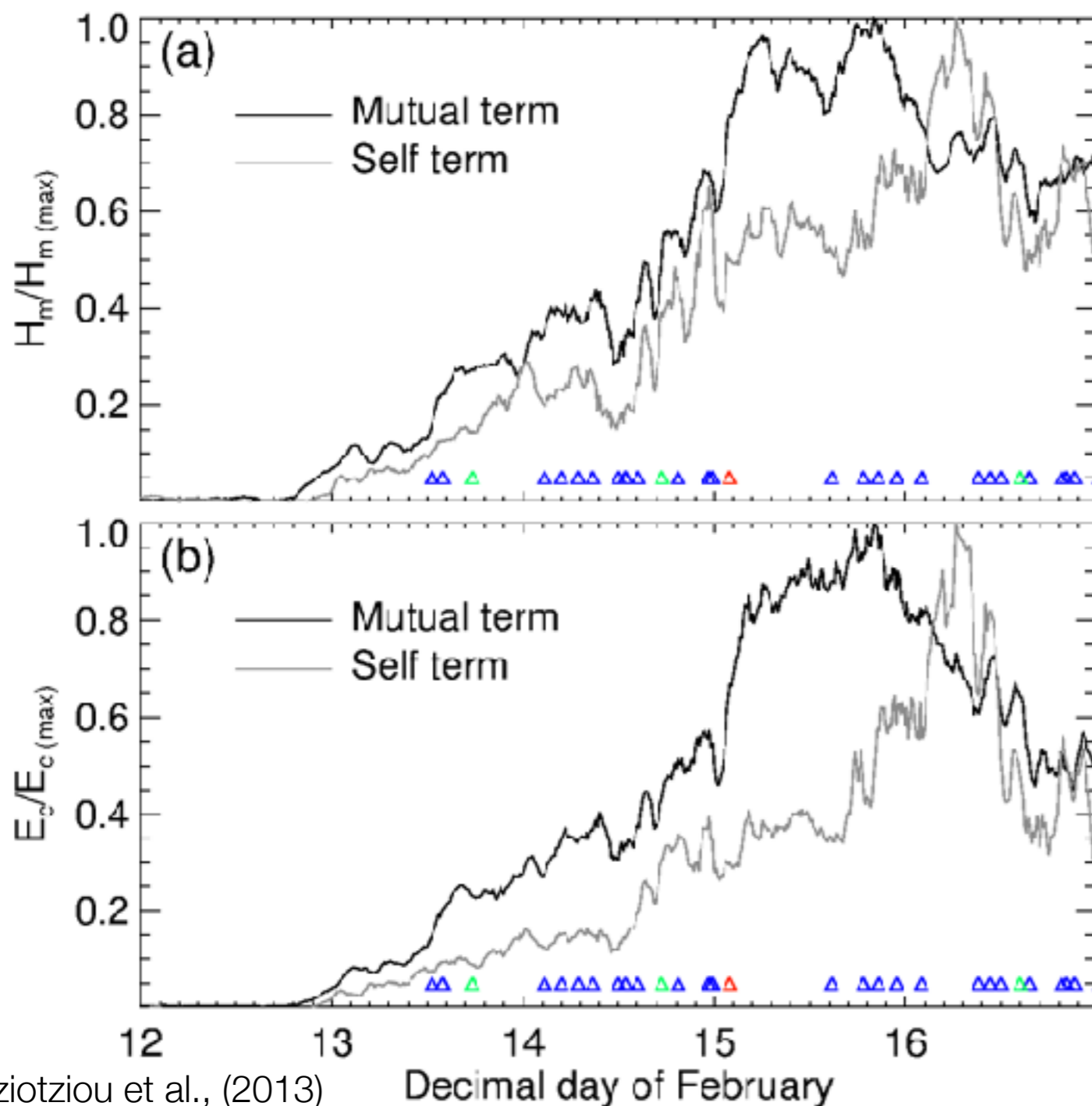


Tziotziou et al., (2013)

Decimal day of February

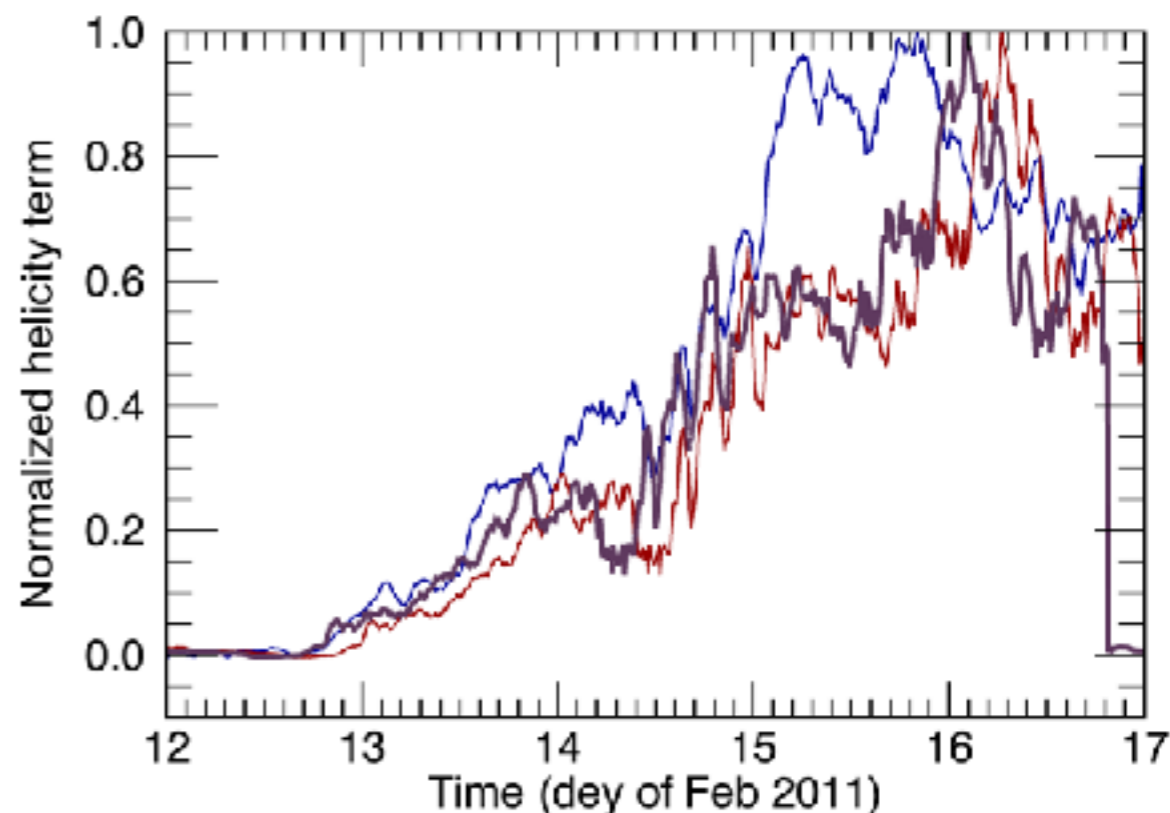
Issues to Work Out. III. Mutual vs. Self Helicity

- Our discrete relative helicity calculation method also enables separation between self and mutual terms of relative helicity and free energy



- Shifting back in time the self helicity timeseries, we can see it shows a hysteresis of ~ 4.4 hours. This does not happen with the free energy.

A case is built, indicating to a self-helicity term due to non-ideal conversion of mutual helicity



Other Helicity Realizations: the “Current-Carrying” Helicity

- The “current-carrying” helicity of Pariat et al., (2017)

$$H_V = H_j + 2H_{pj} \quad \text{with} \quad (9) \quad \text{Relative helicity}$$

$$H_j = \int_{\mathcal{V}} (\mathbf{A} - \mathbf{A}_p) \cdot (\mathbf{B} - \mathbf{B}_p) d\mathcal{V} \quad (10) \quad \text{“Current-carrying” helicity}$$

$$H_{pj} = \int_{\mathcal{V}} \mathbf{A}_p \cdot (\mathbf{B} - \mathbf{B}_p) d\mathcal{V}, \quad (11) \quad \text{Mutual helicity}$$

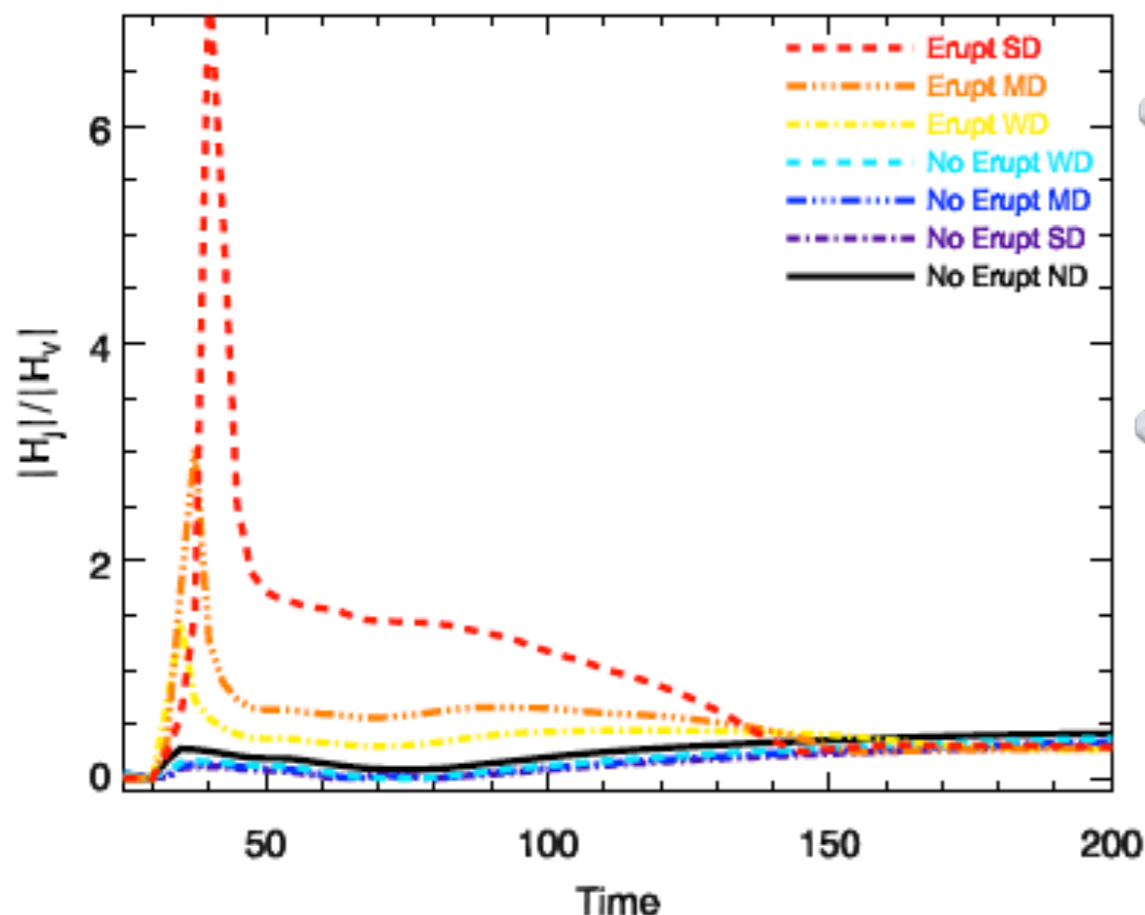
Other Helicity Realizations: the “Current-Carrying” Helicity

- The “current-carrying” helicity of Pariat et al., (2017)

$$H_V = H_j + 2H_{pj} \quad \text{with} \quad (9) \quad \text{Relative helicity}$$

$$H_j = \int_{\mathcal{V}} (\mathbf{A} - \mathbf{A}_p) \cdot (\mathbf{B} - \mathbf{B}_p) d\mathcal{V} \quad (10) \quad \text{“Current-carrying” helicity}$$

$$H_{pj} = \int_{\mathcal{V}} \mathbf{A}_p \cdot (\mathbf{B} - \mathbf{B}_p) d\mathcal{V}, \quad (11) \quad \text{Mutual helicity}$$



- The ratio $|H_j / H_V|$ seems to spike prior to the eruption in the simulation of Leake et al. (2013), implying a possible physical role for H_j
- From its construction and the DeVore gauge ($\mathbf{A} \cdot \mathbf{n} = 0$), H_j does not have a contribution on ∂V and is scale invariant

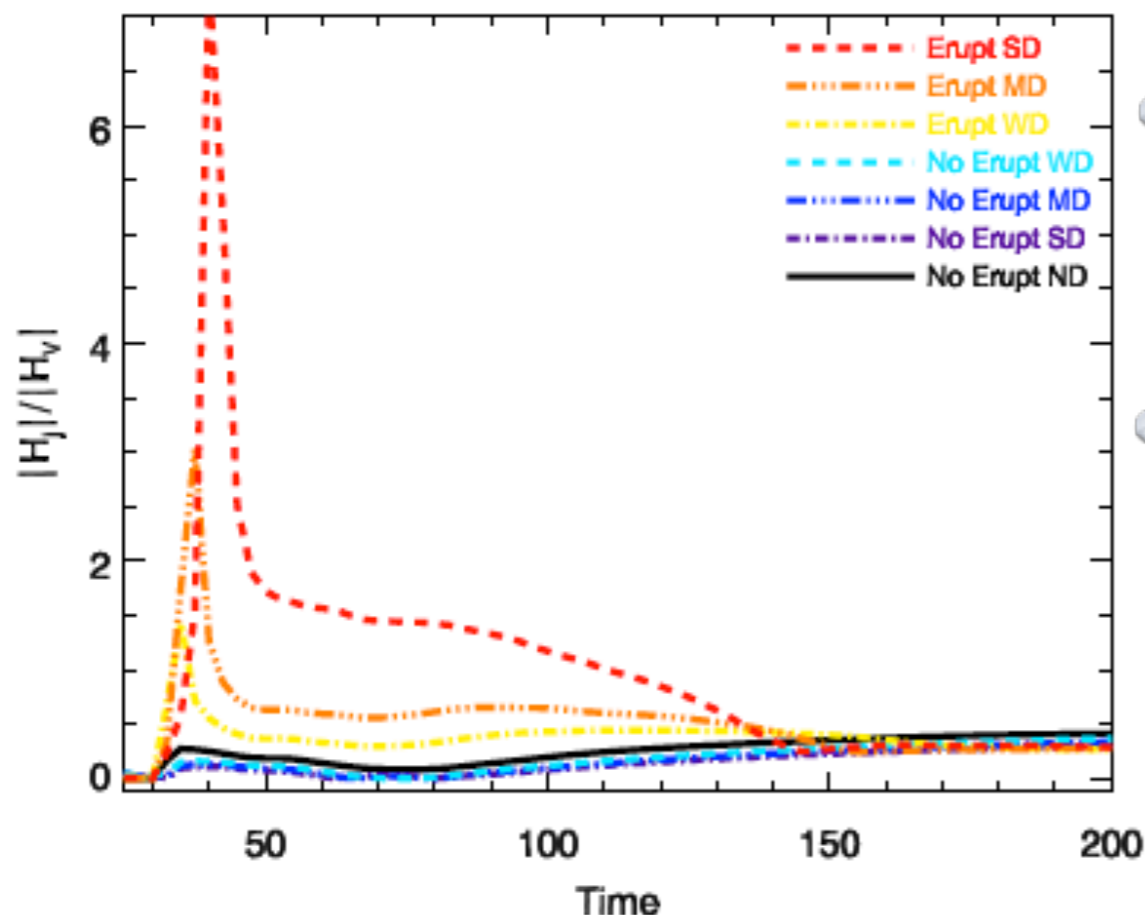
Other Helicity Realizations: the “Current-Carrying” Helicity

- The “current-carrying” helicity of Pariat et al., (2017)

$$H_V = H_j + 2H_{pj} \quad \text{with} \quad (9) \quad \text{Relative helicity}$$

$$H_j = \int_{\mathcal{V}} (\mathbf{A} - \mathbf{A}_p) \cdot (\mathbf{B} - \mathbf{B}_p) d\mathcal{V} \quad (10) \quad \text{“Current-carrying” helicity}$$

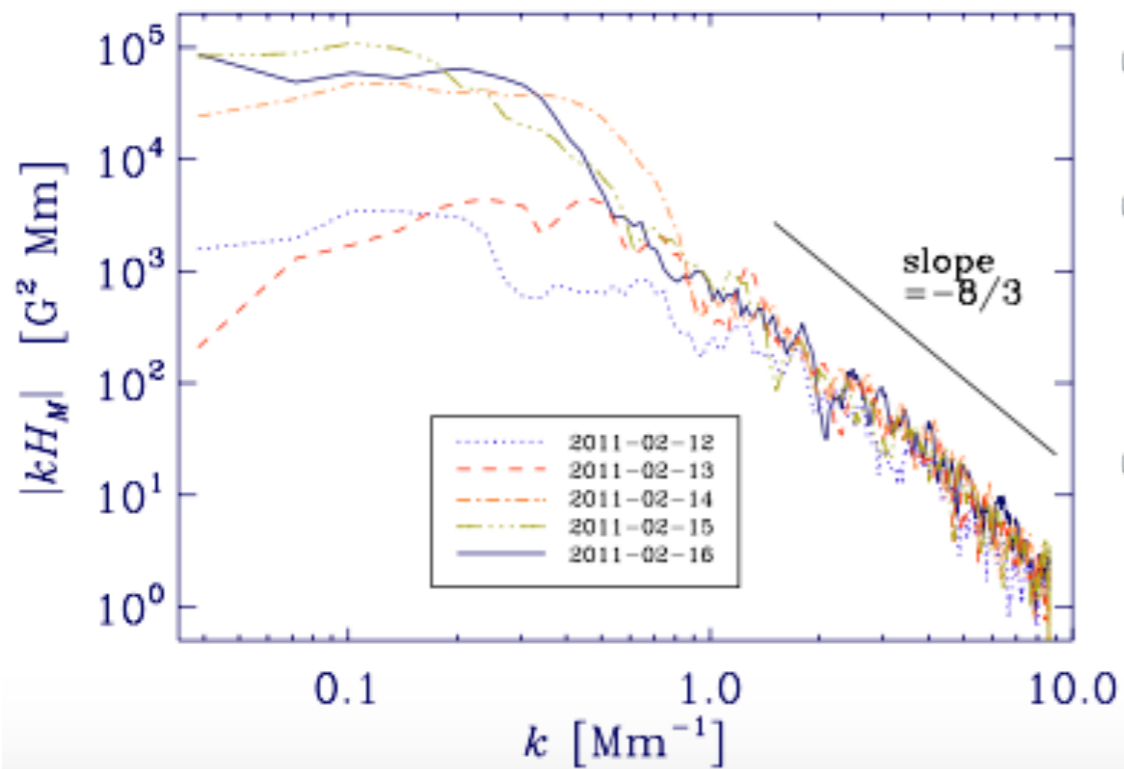
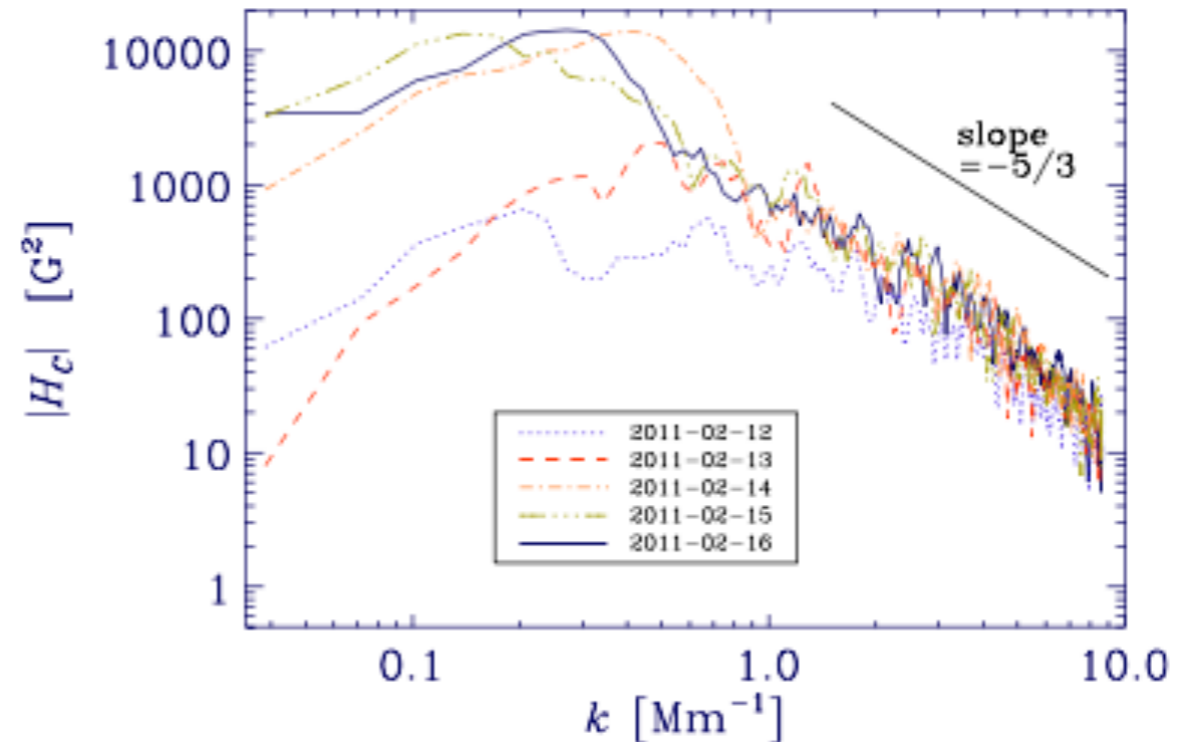
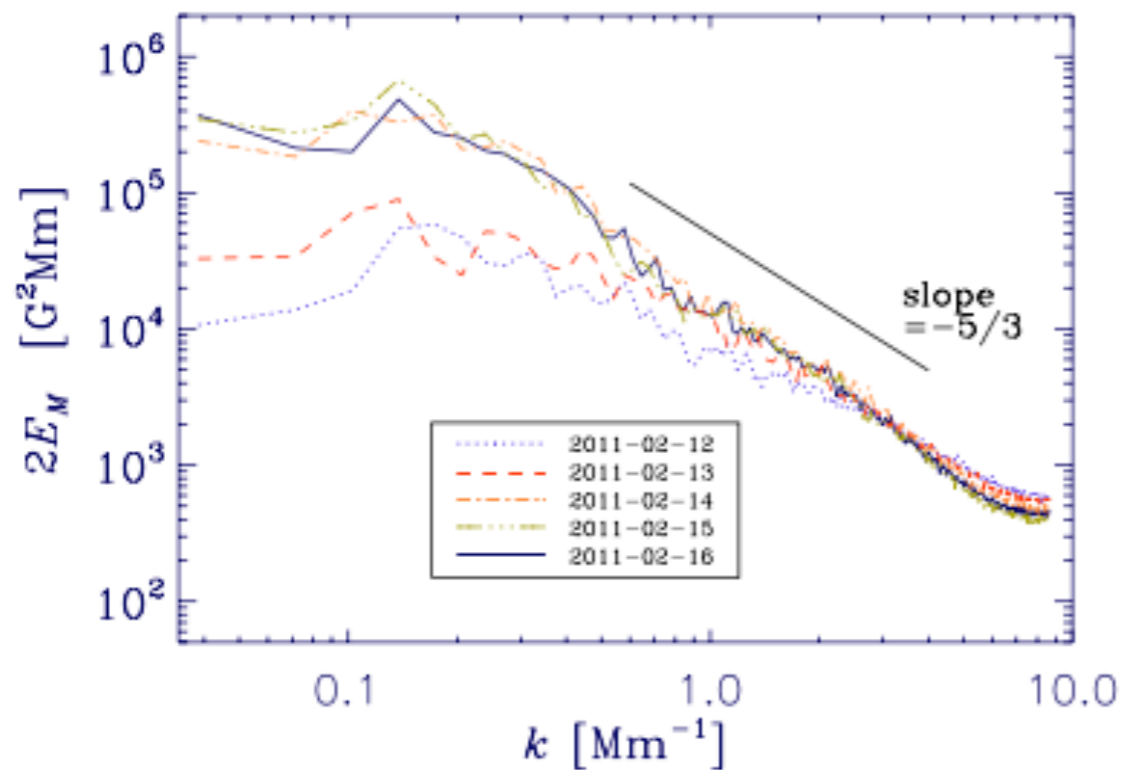
$$H_{pj} = \int_{\mathcal{V}} \mathbf{A}_p \cdot (\mathbf{B} - \mathbf{B}_p) d\mathcal{V}, \quad (11) \quad \text{Mutual helicity}$$



- The ratio $|H_j / H_V|$ seems to spike prior to the eruption in the simulation of Leake et al. (2013), implying a possible physical role for H_j
- From its construction and the DeVore gauge ($\mathbf{A} \cdot \mathbf{n} = 0$), H_j does not have a contribution on ∂V and is scale invariant

More work is needed to understand H_j better

Finally, the Helicity Spectra



- NOAA AR 11158
- Realizability condition: $k|H(k, t)| \leq 2E(k, t)$
(constraining magnetic helicity, albeit in Fourier space)
- First complete calculation of the current helicity, albeit in Fourier space

$$H_c(k, t) \simeq k^2 H(k, t)$$

Hoping to hear more in this Thinkshop!

Zhang, Brandenburg & Sokoloff (2014, 2016)

Conclusions

- Ground-breaking progress in solar magnetic helicity studies over recent decades
- [Relative] magnetic helicity is now placed on equal footing with [free] magnetic energy in solar low-atmospheric configurations
- As in every such progress, however, more questions than answers are borne. In particular:

Conclusions

- Ground-breaking progress in solar magnetic helicity studies over recent decades
- [Relative] magnetic helicity is now placed on equal footing with [free] magnetic energy in solar low-atmospheric configurations
- As in every such progress, however, more questions than answers are borne. In particular:
 - We need to make sense / correlate between different helicity “flavors”: relative (magnetic), “current-carrying”, “spectral”, current, kinetic, quadratic, cross-helicity, etc.
 - We need to understand the interplay between the two different senses of magnetic helicity in the same magnetic structure.
 - We need to understand the interplay between the mutual and self-helicity in emerging magnetic structures.
 - Coherence of active-region helicity (deep-seated) vs. randomness of QS helical patterns (near-surface[?])

Thank you!

ありがとう

